A Distinctive Example of the Cooperative Interplay of Structure and Environment in Tuning of Intramolecular Charge Transfer in Second-Order Nonlinear Optical Chromophores

Alessandro Abbotto,*[a] Luca Beverina,[a] Silvia Bradamante,[b] Antonio Facchetti,[a] Christopher Klein,[c] Giorgio A. Pagani,*[a] Mesfin Redi-Abshiro,[c] and Rüdiger Wortmann[c]

Abstract: The strongly enhanced cooperative influence of medium polarity and organic structural design on the first hyperpolarizability β of a novel family of highly polarizable azinium-(CH=CH-thienyl)-dicyanomethanido chromophores **1 – 3** is described. The dyes can be efficiently synthesized by regioselective protonation/alkylation of the corresponding bidentate anion precursors. Consecutive annelation of the pyridyl ring of **1** (pyridine → quinoline → acridine) and medium polarity effects are responsible for an extraordinarily variable range of intramolecular charge transfer (ICT), leading to a large set of π-electron distribution patterns. Accordingly, systems with remarkably different zwitterionic/quinoid character in the ground and excited states present β values in a broad range, eventually switching from negative to positive. Our investigation is based on a combination of experimental (UV/Vis spectroscopy, multinuclear NMR spectroscopy, and electrooptical absorption measurements) and computational (ab initio) approaches. It is shown that: 1) β and $\mu\beta$ are dramatically influenced, even by orders of magnitude, by a complex, non-monotonic interplay of structure and medium action, which in turn affects molecular ICT and bond length alternation (BLA), 2) the computations, validated by different experimental data, are to be recommended as an extremely useful tool in the search for a greatly improved set of molecular nonlinear optical (NLO) responses (in the case of **1 – 3** they show that such conditions may be attained only in a narrow and limited range of dielectric constants in which the annelation effect operates most efficiently), and 3) the search for the most favorable molecular NLO response of a highly polarizable chromophore both in solution and in solid matrices should simultaneously take into account not only the molecular design supplemented by annelation effects but also the polarity of the medium.

Keywords: ab initio calculations · annelation · heterocyclic zwitterions · NMR spectroscopy · nonlinear optics

[a] Prof. Dr. A. Abbotto, Prof. Dr. G. A. Pagani, Dr. L. Beverina,
Dr. A. Facchetti
Department of Materials Science and INSTM
University of Milano-Bicocca, Via Cozzi 53
20125 Milano (Italy)
Fax: (+39) 02-64485403
E-mail: alessandro.abbotto@unimib.it, giorgio.pagani@unimib.it

[b] Dr. S. Bradamante
CNR-Institute of Molecular Sciences and Technologies
Via Golgi 19, I-20133, Milano (Italy)

[c] C. Klein, M. Redi-Abshiro, Prof. Dr. R. Wortmann
Department of Physical Chemistry
University of Kaiserslautern
Erwin-Schroedinger-Strasse, 67663, Kaiserslautern (Germany)

Supporting information for this article is available on the WWW under http://www.chemeuj.org or from the author. UV/Vis spectra of **1a, 1b**, **2a, 2b** and **3a** in different solvents (Figures S1 – S5); optical and electrooptical absorption spectra of **1b** and **2b** in dioxane (Figures S6 and S7); computed structures of **1c – 3c** in dioxane and chloroform (Figures S8 and S9); table of computed energies (Table S10); plot of β_0 against ε (Figure S11); x,y,z coordinates of all structures.

Introduction

The electronic and structural properties of organic push – pull conjugated compounds are of considerable interest for nonlinear optical (NLO) applications in photonic and electrooptic devices such as high-speed photonic switching and electrooptic modulators.[1] To generate highly efficient NLO-phores with a large quadratic hyperpolarizability β, extensive molecular polarization of the π-electron structure is usually provided by means of a strong interaction between end-capped donor and acceptor groups. This situation gives rise to a dominant intramolecular charge-transfer (ICT) transition from the ground state (g) to their first excited state (e). The sign and value of β have been correlated with the bond length alternation (BLA)[2] structural parameter, whereas other authors have correlated β, through the two-state model, to other expressions such as $c^{2[3]}$ and MIX.[4] All three descriptors are correlated between themselves.[4] In the plot of β against BLA it has been shown that in push – pull polyenes β moves

from positive (BLA < 0, neutral ground state) to negative (BLA > 0, dipolar ground state), with values passing through zero (BLA = 0, cyanine limit).[5]

We have reported the synthesis of a novel series of chromophores[6] **A** endowed with solvent-dependent, very large, and negative $\mu\beta$ values (Scheme 1).[7] Indeed, the solvent polarity has been shown both theoretically[8] and experimentally[9] to have a great influence on ICT, and thus on β. Changing the strength of the donor and the polarity of the solvent β can even change the sign.
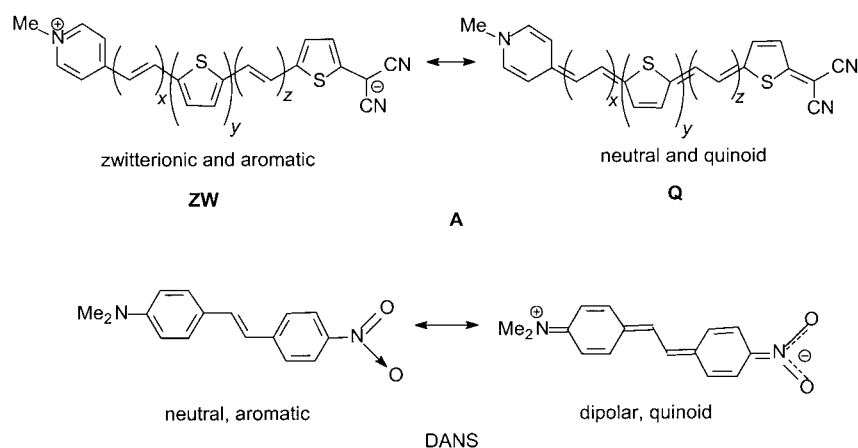
Scheme 1. Resonance between zwitterionic/aromatic – neutral/quinoid (system **A**) and neutral/aromatic – dipolar/quinoid (DANS-like systems) limit forms.

Our molecular design approach was based on the following main strategic choices:

1) Exploitation of π-excessive and π-deficient heteroaromatic compounds[10] as key constituent donors and acceptors of the push–pull NLO-phore.[11] Theoretical and experimental studies have demonstrated that π-excessive and π-deficient heterocycles can efficiently function as primary[11] and/or auxiliary[12] donor and acceptor groups in push–pull dyes; furthermore, the reduced ring aromaticity relative to benzene of the five-membered heterocycles leads both to an increased transition moment and to change in dipole moment.[13]

2) In contrast to the most common approach in the literature (e.g., for 4-dimethylamino-4′-nitrostilbene DANS, Scheme 1), the dipolar (zwitterionic) limit formula retains aromaticity, whereas the neutral limit formula is quinoid.[14]

We realized, however, that for the above zwitterions, both the large solvatochromic response and the highly solvent-dependent $\mu\beta$ values, which increase as the solvent polarity decreases, needed a rationale. This prompted us to investigate the solvent response of the zwitterionic systems more closely, and in this we were strongly supported by our recent experimental findings that the solvent modulates[15] the extent of ICT within a series of pyridine-based systems. We thus decided to obtain $\mu\beta$ values in a solvent possessing a dielectric constant ε definitely lower than those of the previously considered solvents (DMF and CHCl$_3$). Preliminary experiments convinced us that EFISH (electric-field-induced second harmonic) generation[1] experiments were not viable

because of the extremely low solubility of the zwitterions of type **A**—that in all cases retain highly polar natures—in any solvent of low polarity. The EOAM (electrooptical absorption measurements) approach[16, 17] seemed practicable since the measurements can be obtained at concentrations typical of UV/Vis absorption spectroscopy. In addition, we felt it might be profitable to carry out ab initio computations that, by taking into account of the solvent effects, could mimic the contributions of the dipolar and zwitterionic structures in the different environments.

Since, on the whole, the combination of BLA, which strictly depends upon the π-electron structure, and of the solvent influences the change in the relative contributions of the two neutral and dipolar limit forms of the chromophore ground and excited states, we decided, taking the zwitterion **1a** (see Scheme 2) as a starting point, to extend the investigation to very similar systems presenting in their structures other acceptor groups, but ones with small or negligible variation in their electron-withdrawing capacities and that would in turn be able to influence the BLA on the basis of bond localization only. We took the decision, unprecedented in the literature, to use benzofusion (*annelation effect*)[18] of the acceptor pyridinium ring as a regulator of π-delocalization. Accordingly, we prepared and characterized chromophores **1–3** and, to address solubility problems, also planned the synthesis of the type **b** N-decyl-substituted chromophores (Scheme 2). Indeed, Scheme 3 shows that the bond lengths of the bonds from the pyridyl-nitrogen atom to the position at which the double bond in **1–3** is joined show considerable alternation. Thus, consecutive annelation of pyridine with one and then with two benzene rings in **1–3** can cause significant bond alternation and would be expected to influence the relative importance of the aromatic/quinoid character of the azinium ring, thus affecting the entire π framework.

Scheme 2 clearly shows that, whereas the pyridine ring loses aromaticity in the right-hand side formula, the acridinium ring can better sustain a quinoid character thanks to the restored full aromaticity of the two benzene side rings. The quinolinium ring is somewhere in the middle. It is therefore to be expected that in the ground state the importance of the **ZW** form should sequentially decrease, and the **Q** form simultaneously increase, on going from pyridine to quinoline to acridine. To the best of our knowledge the annelation effect has never been used as a structural tool for affecting the relative contribution of the two limit forms, but the acridine ring was also never reported as an acceptor moiety in NLO dyes. Indeed, the quinolinium ring has hardly appeared in the NLO literature[14d, 19] and in none of these cases did the authors mention the annelation effect as a precise tool for designing new dyes with optimized values of β.
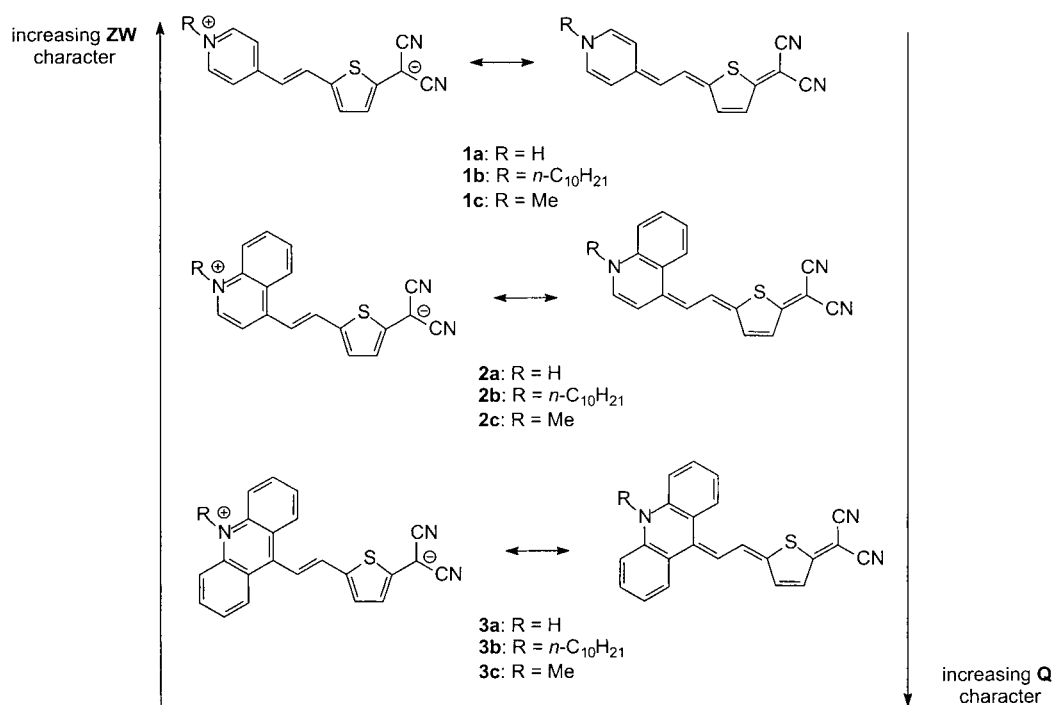
Scheme 2. Effect of annelation of the pyridine ring on the contribution of the zwitterionic/aromatic (**ZW**) and neutral/quinoid (**Q**) resonance structures in the description of the ground state.
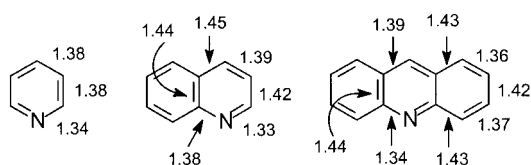
Scheme 3. Bond lengths [Å] in pyridine, quinoline, and acridine (averages of different X-ray data reported in the literature for alkyl derivatives).

In short, for the detailed investigation of systems **1–3** we will use a combination of a number of approaches, very different in nature and targets: organic design and synthesis, multinuclear NMR investigation to provide insights into charge-mapping and bond length alternation, linear absorption, EOA measurements in 1,4-dioxane for comparison with and discussion of previous measurements in solvents of higher polarity, and computational (ab initio) investigation, with effects of the medium always included. We will show that the successive steps we propose herein—molecular design including annelation effects and choice of the medium—can provide an extremely variable (to the extent of *orders of magnitude)* set of β values. We believe that the procedure outlined herein provides an unprecedented novel methodology to access optimized NLO properties.

## Results

Synthesis of chromophores

The synthesis of chromophores **1** and **2** are reported in Scheme 4 and that of chromo-

phore **3** is reported in Scheme 5. Bromo derivatives **7** and **8** are new compounds. Compound **7** was prepared by a Horner–Wittig reaction between the diethyl[(5-bromothien-2-yl)methyl]phosphonate anion and 4-formylquinoline in THF. Condensation of 4-methylacridine (**9**) with 5-bromo-2-formylthiophene in AcONa/AcOH solution afforded **8** as a mixture of the *E* and *Z* geometric isomers. This result is surprising in view of the large steric hindrance experienced by the *cis* diastereoisomer. Isomers (*E*)-**8** and (*Z*)-**8** can conveniently be separated by column chromatography.

In a previous paper[6] we described the preparation of sodium salt **4**. Similarly, **5** and **6** were synthesized from the parent bromothiophenes **7** and **8**, respectively, by treatment with malonodinitrile sodium salt in dimethoxyethane, with tetrakis(triphenylphosphine)palladium(0) as catalyst. Note that both (*E*)-**8** and (*Z*)-**8** diastereoisomers react with malonodinitrile sodium salt to afford the same product (*E*)-**6** (Scheme 6). It is likely that each bromo isomer gives the
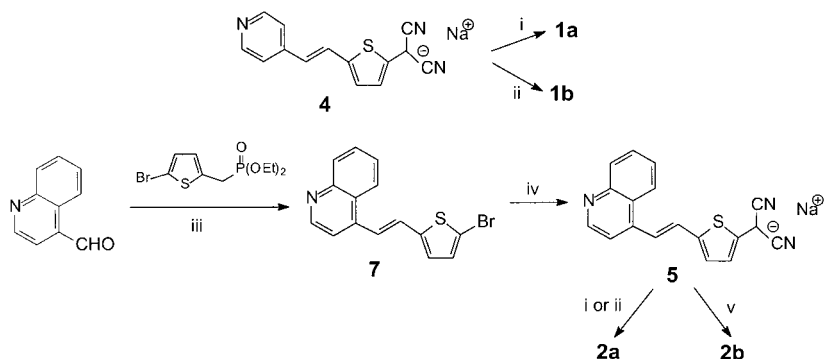
Scheme 4. Synthesis of pyridine chromophores **1a** and **1b** and quinoline chromophores **2a** and **2b**: i) HCl, DMSO; ii) CF$_3$SO$_3$C$_{10}$H$_{21}$, acetone, RT; iii) NaH, THF, reflux; iv) CH$_2$(CN)$_2$, NaH, DME, [Pd(PPh$_3$)$_4$], RT; v) CF$_3$SO$_3$C$_{10}$H$_{21}$, K$_2$CO$_3$, CH$_3$CN, Δ.
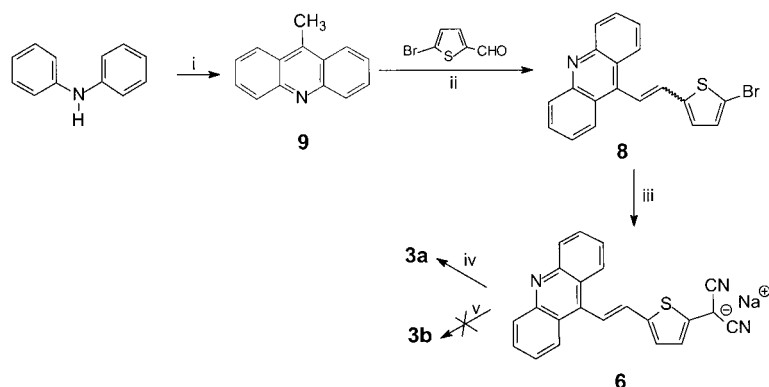
Scheme 5. Synthesis of the acridine derivative **3a** and failure to prepare **3b**: i) AcOH, ZnCl₂, 200 °C; ii) AcOH, AcONa, 130 °C; iii) CH₂(CN)₂, NaH, DME, [Pd(PPh₃)₄], RT; iv) HCl, DMSO; v) CF₃SO₃C₁₀H₂₁, different conditions.
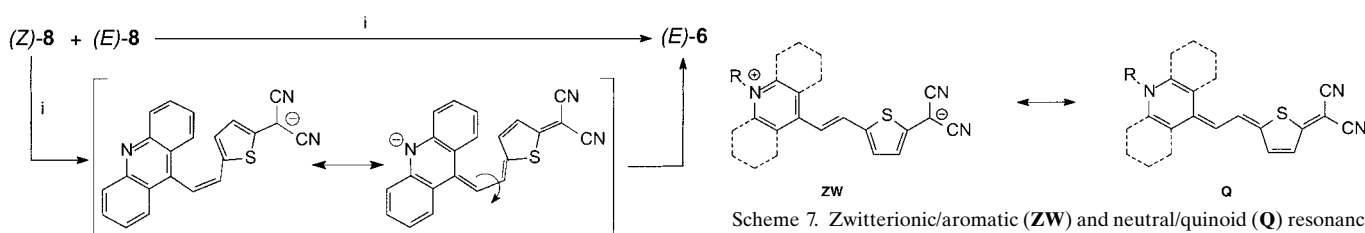
Scheme 6. Preparation of the *E* diastereoisomer of the acridine-based sodium salt **6** from both the *E* and the *Z* forms of the precursor bromo derivative **8**: i) CH₂(CN)₂, NaH, DME, [Pd(PPh₃)₄], RT.

corresponding sodium salt and that (*Z*)-**6** only subsequently isomerizes to (*E*)-**6**.

Finally, the last synthetic step to prepare dyes **1**–**3** was designed on the basis of our previous experience on bidentate anions. All chromophores **1a**–**3a** were conveniently prepared in high yields (> 80 %) by regioselective nitrogen protonation of anions **4**–**6** with 10 % hydrochloric acid. Among the *N*-alkyl substituents we made use of a medium-length chain to improve the solubility of the final zwitterions **1**–**3**. The sodium salts **4**–**6** exhibit different behavior toward alkylation with alkyl triflates. In fact, while the reaction between **4** and CF₃SO₃C₁₀H₂₁ took place efficiently and in high yield, compound **5** reacted less easily and **6** did not at all. Compound **1b** was prepared in acetone, but sodium salt **5** afforded **2a** under the same conditions. Probably the quinoline nitrogen atom is less reactive and so the alkyl triflate has time to react with acetone to form triflic acid, which protonates **5** to give **2a**. To avoid this inconvenience, the alkylation reaction was carried out in acetonitrile and in the presence of K₂CO₃. Compound **2b** was isolated in pure form after column chromatography. All attempts to prepare **3b** with different alkylation reagents and/or under different experimental conditions failed. However, the fact that **3b** was not available does not constitute a problem: compound **3a** is fortunately soluble enough and the optical properties of the series **1/2** (**a**) are indistinguishable from those of series **1/2** (**b**).

Solvatochromic data

Both the ground and the excited states of molecules **1**–**3** can be represented as linear combinations of the zwitterionic

(**ZW**) and quinoid (**Q**) limit resonance formulas, and the solvatochromic effect—defined as the dependence of the dyes' UV/Vis absorption spectra on solvent polarity—is a useful method for investigating their nature. Depending on chromophore structure and solvent polarity,[20] one of the two limit formulas will be more suitable to describe the chemical bonding of the real molecule in the two states (Scheme 7).

Each of the chromophores **1**–**3** presents a strong charge-
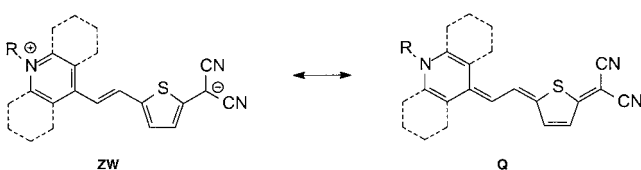
Scheme 7. Zwitterionic/aromatic (**ZW**) and neutral/quinoid (**Q**) resonance structures of chromophores **1**–**3**.

transfer (CT) band in the visible region of the spectrum. Table 1 lists absorption data (λ_max) relative to the CT band in selected solvents (the corresponding spectra can be found in the Supporting Information; Figures S1–S5). Maximum wavelength values listed in Table 1 are taken at the local maximum of the lowest energy band, on the assumption that this band should refer to the monomeric species.[21] A recent investigation into the aggregation of merocyanine dyes has shown that the band of lowest energy can be ascribed to the monomers, with subsidiary vibronic maxima or shoulders at shorter wavelengths; dye aggregates are hypsochromically shifted with respect to the monomer.[22]

If the molecular ground state is better described by **ZW**, the charge-transfer direction is from the negatively charged dicyanomethanido moiety to the *N*-alkylazinium group. The other possibility, envisioned when **Q** is the better ground state descriptor, is from the aminoquinoid group to the dicyanovinyl acceptor. The first situation gives rise to a negative solvatochromic response, which becomes positive in the latter case.

Table 1. Solvatochromic data[a] (λ_max [nm] of the charge-transfer band) for the chromophores **1a**–**3a**, **1b**, and **2b** in selected solvents.

Compound (ε)	DMSO (46.7)	Acetone (20.7)	THF (7.6)	CHCl₃[b] (4.8)	Dioxane[b] (2.2)	Δλ
1a	608	635	676	684	709	− 101
1b	619	645	686	702	708	− 89
2a	697	723	739	746	748	− 51
2b	714	738	758	765	763	− 49
3a	787	678	672	658	630	+ 157

[a] Δλ = λ_max(DMSO) − λ_max(dioxane); positive Δλ values mean positive solvatochromism. [b] The lowest energy transition was considered.

Multinuclear NMR investigation

^{13}C and ^{15}N NMR data: Theoretical studies have shown the strict correlation between molecular NLO activity and charge distribution on the donor, spacer, and acceptor chromophore groups.[8b, 23] We had previously proposed,[24] and confirmed,[25] the validity of empirical π-electron/shift relationships [Eq. (1) and Eq. (2)] to correlate the variation of the π electron density on sp^2 carbon and nitrogen atoms with variation of the corresponding chemical shift.

$$\Delta\delta(^{13}C) = -160\Delta q_C^{\pi} \tag{1}$$

$$\Delta\delta(^{15}N) = -366.34\Delta q_N^{\pi} \tag{2}$$

The ^{13}C and ^{15}N NMR shifts (Figure 1) therefore allow a map of charge distribution on the chromophore structure in solution to be drawn and could, for the first time, provide a useful experimental correlation between π-charge and NLO activity.

^{1}H NMR data: ^3J(H,H) coupling constants are particularly sensitive to H-C-C-H bond lengths, angles, and carbon hybridization: in short, to molecular structure.[4b, 26] Combined theoretical and NMR investigations on cyanine, merocyanine, and polyenes dyes have shown a clear correlation between the coupling constant of *trans* vicinal protons in the conjugated chain and the corresponding C−C bond order.[27] In addition, solvent-dependent NMR studies conducted on push–pull polyenes suggested that the ground-state structure can be significantly affected by solvent polarity.[4c, 28] Therefore, the coupling constants of dyes **1**–**3** in general, and ^3J of the π-bridge in particular, would be expected to vary on going from a **ZW** to a **Q** limit structure (Scheme 8).
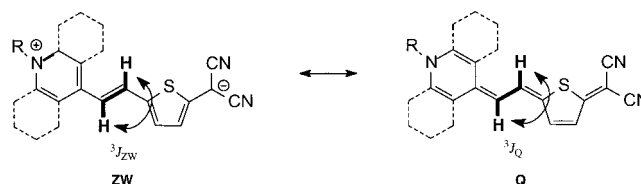
Scheme 8. Use of the ^3J(H,H) coupling constant of the central ethenylic unit of chromophores **1**–**3** to monitor the different contributions of the zwitterionic/aromatic (**ZW**) and neutral/quinoid (**Q**) resonance structures to the description of the ground state.

Proton NMR spectra of compounds **1b**, **2b**, and **3a** were recorded in solvents of different polarities. We chose deuterated dimethyl sulfoxide, chloroform, and dioxane: their corresponding protonated analogues have dielectric constant ε values of 46.7, 4.80, and 2.21, respectively. By this approach it is possible to analyze: 1) whether the ground state chemical representation of dyes **1**–**3** is closer either to the **ZW** or to the **Q** structure in that particular environment, and 2) the sensitivity of each structure to solvent polarity.

Figure 2 shows ^{1}H NMR spectra of **1b** in these three solvents. Table 2 lists ^3J(H,H) values for the chromophores under investigation in selected solvents. Considering the same chromophore system, and therefore looking at Table 2 along the rows, it can be noted that a decrease in solvent polarity is concomitant with a decrease in the ^3J(H,H) coupling constant. This result suggests the conclusion that the double-bond character of the π bridge is reduced, indicative of an increased contribution of the quinoid limit formula. This change is larger for the pyridine-based system (Δ^3J(H,H) = 1.51 Hz) than for the quinoline- (Δ^3J(H,H) = 1.31 Hz) and acridine-based (Δ^3J(H,H) = 1.07 Hz) systems. Alternatively, when the same solvent is considered, ^3J(H,H) (**1**) > ^3J(H,H) (**2**) > ^3J(H,H) (**3**), showing that the pyridine-based system **1** is always more zwitterionic than **2**, while **3** has the most quinoid character *in all solvents*.

A further remarkable result is that a drastic change in the chemical shifts is recorded on going from DMSO to less polar solvents. Pyridine protons shift upfield by about 1 ppm on going from DMSO to CDCl$_3$/dioxane, meaning that they move
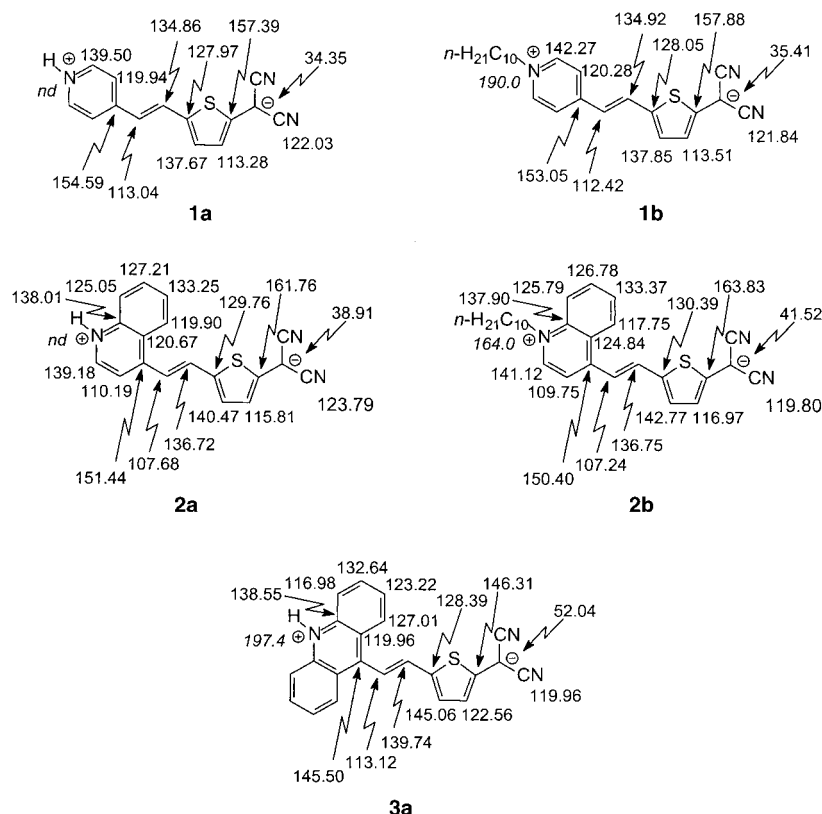

Figure 1. ^{13}C and ^{15}N (italics) NMR data in DMSO at 27 °C for compounds **1a**–**3a**, **1b** and **2b**; *nd* means that the signal was not detected.
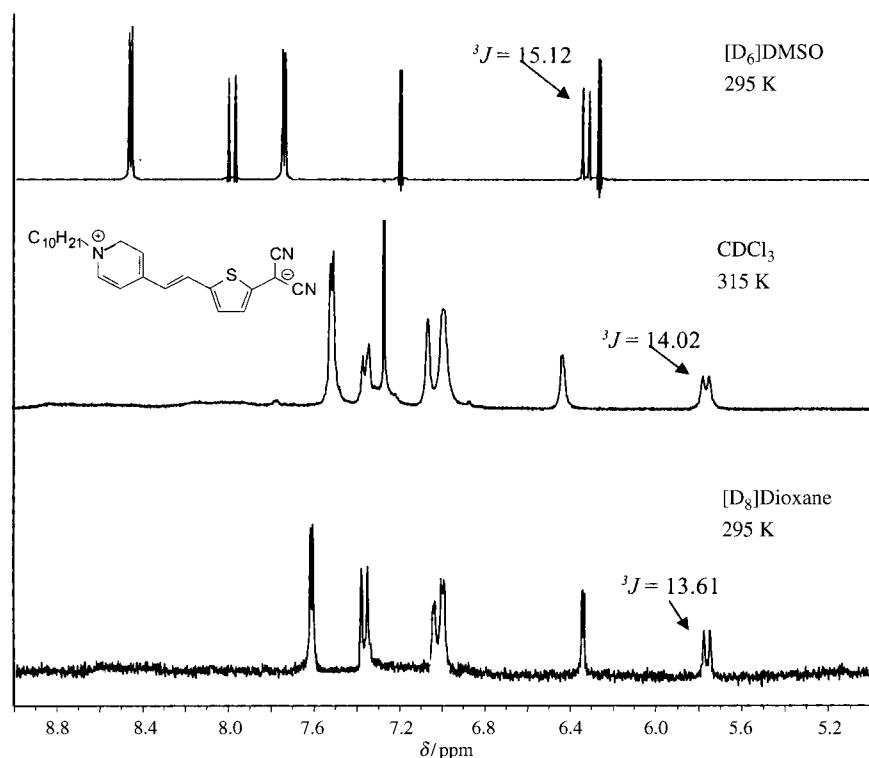
Figure 2. ^{1}H NMR spectra of **1b** in [D$_6$]DMSO, CDCl$_3$, and [D$_8$]dioxane at 25 °C (aromatic region).

Table 2. Solvent-dependent ^{1}H NMR coupling constants [Hz] of the central ethenylic unit in systems **1–3**.[a]

Compound	Dioxane	CHCl$_3$	DMSO
1b	13.61	14.02	15.12
2b	12.99	13.42	14.33
3a	12.69	12.78	13.76

[a] Measured at 298 K.

from a typical pyridinium salt environment to a more quinoid-like structure. In addition, while the DMSO spectrum exhibits very sharp signals, the dioxane and CDCl$_3$ spectra are somewhat broader. This result can be explained by assuming completely free rotation about the C–C bonds adjacent to the C=C in a zwitterionic-like structure (DMSO), whereas an equilibrium between different rotamers can be envisioned in a quinoid-like structure (CDCl$_3$, dioxane). Another possibility could be due to the formation of molecular aggregates, a known phenomenon[29] more likely in nonpolar or weakly polar solvents. A similar trend, but more attenuated, can be observed for all of the other chromophores.

Electrooptical and nonlinear-optical properties

Optical absorption spectra of donor—acceptor-substituted π systems typically show a single intense charge-transfer (CT) transition at low energy. A powerful experimental technique with which to characterize these CT transitions is electro-optical absorption (EOA) spectroscopy.[16, 17] In this work we have utilized this technique to determine the ground and excited state dipole moments of the chromophores **1b**, **2b**,

and **3a** and to analyze the resonance structures of the chromophores in terms of the **Q** and **ZW** limit contributions.

The EOA technique measures the influence of the square of an external electric field on the molar decadic absorption coefficient according to Equation (3), where ε^E is the absorption coefficient in the presence of the electric field E.

$$\varepsilon^E(\phi, \tilde{\nu}) = \varepsilon(\tilde{\nu})[1 + L(\phi, \tilde{\nu})E^2 + \ldots] \qquad (3)$$

The relative change induced by the field L is a function of the wavenumber $\tilde{\nu} = 1/\lambda$ and the angle ϕ between the polarization vector of the incident light and the applied field. Typically the EOA spectrum is recorded for two polarizations $\phi = 0°$ and 90°, and multilinear regression analysis in terms of the optical absorption spectrum and its first derivative yields a set of regression coefficients D, E, F and G, from which the ground state dipole moment μ_g and the dipole difference $\Delta\mu$ between the ground state (g) and the excited state (e) may be calculated.[30] An important additional quantity is the magnitude of the transition dipole moment μ_{eg}, which may be determined from the integrated absorption spectrum. It has been demonstrated in a series of papers[3, 31] that knowledge of $\Delta\mu$, μ_{eg} and of the wavelength of optical excitation (λ_{eg}) of the CT transition obtained from UV/Vis and EOA spectra allows the static second order polarizability β_0 [Eq. (4)] and the anisotropy of the first order polarizability $\delta\alpha_0$ of the dye to be estimated in a two-level model [Eq. (5)].

$$\beta_0 = \frac{6\mu_{eg}^2 \Delta\mu \lambda_{eg}^2}{(hc)^2} \qquad (4)$$

$$\delta\alpha_0 = \frac{2\mu_{eg}^2 \lambda_{eg}}{(hc)} \qquad (5)$$

Furthermore, EOA results allow us to analyze the resonance structure of the chromophores in a simple CT model, which describes the ground and excited states as linear combinations of the **Q** and **ZW** limit structures on the basis of the resonance parameter c^2. According to this simple model, donor—acceptor-substituted π-conjugated chain molecules may be classified from polyene-type ($c^2 \approx 0$) through neutro-cyanines ("cyanine limit", $c^2 \approx 0.5$) to zwitterionic systems ($c^2 \approx 1$). The implications of this classification for the optimization of chromophores for nonlinear-optical and photo-refractive applications have been discussed in a number of publications.[32] A further parameter of this model is the maximal hypothetical dipole change $\Delta\mu_{max}$: the difference of

the dipole moments of the **Q** and the **ZW** structures. The model parameters c^2 and $\Delta\mu_{max}$ can be estimated from Equation (6) and Equation (7)

$$c^2 = 1/2\,[1 - \Delta\mu(4\mu_{eg}^2 + \Delta\mu^2)^{-1/2}] \tag{6}$$

$$\Delta\mu_{max} = \Delta\mu/(1 - 2c^2) \tag{7}$$

Figures S6 and S7 in the Supporting Information and Figure 3 display the EOA spectra of **1b**, **2b**, and **3a**, respectively, and Table 3 summarizes all EOA results. Because of partial aggregation (dimer formation) of **1b** and **2b** in
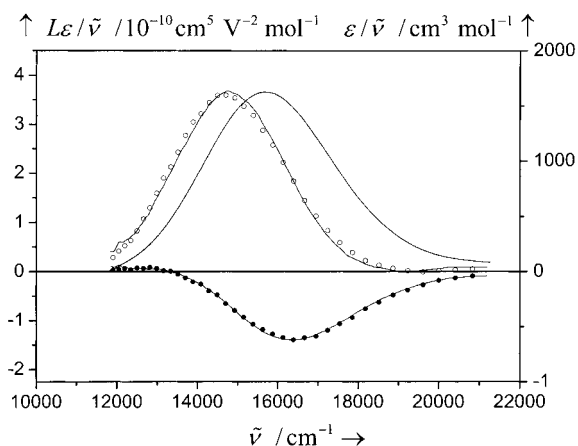

Figure 3. Optical ($\varepsilon/\tilde{\nu}$) and electro-optical absorption spectra ($L\varepsilon/\tilde{\nu}$) of **3a** in dioxane, $T = 298$ K. Data points for parallel ($\circ$: $\phi = 0°$) and perpendicular polarisation ($\bullet$: $\phi = 90°$) of the incident light relative to applied electric field and multilinear regression curves.

Table 3. Results of electrooptical absorption measurements in dioxane ($T = 298$ K) and derived nonlinear-optical properties of **1b**, **2b**, and **3a**.

Parameter units		Compound		
		1b	**2b**	**3a**
D	$[10^{-20}\,V^{-2}m^2]$	7820 ± 530	3660 ± 430	300 ± 90
E	$[10^{-20}\,V^{-2}m^2]$	$118\,500 \pm 3100$	$80\,400 \pm 2700$	$26\,500 \pm 540$
F	$[10^{-40}\,C\,V^{-1}m^2]$	-2780 ± 620	1170 ± 580	7090 ± 390
G	$[10^{-40}\,C\,V^{-1}m^2]$	-2860 ± 620	1780 ± 580	7430 ± 390
λ_{eg}	[nm]	708	763	630
ε	$[m^2mol^{-1}]$	–	–	3410
μ_{eg}	$[10^{-30}\,C\,m]$	37.0	36.8	31.6
μ_g	$[10^{-30}\,C\,m]$	66.7 ± 1.1	56.2 ± 1.1	32.7 ± 0.5
$\Delta\mu$	$[10^{-30}\,C\,m]$	-8.9 ± 1.1	5.5 ± 1.5	46.7 ± 1.9
μ_e	$[10^{-30}\,C\,m]$	57.8 ± 1.8	61.7 ± 1.8	79.3 ± 1.8
$\Delta\alpha_0$	$[10^{-40}\,C\,V^{-1}m^2]$	98	104	69
β_0	$[10^{-50}\,C\,V^{-2}m^3]$	-92 ± 15	66 ± 18	338 ± 14
c^2		0.56 ± 0.01	0.46 ± 0.01	0.20 ± 0.01
$\Delta\mu_{max}$	$[10^{-30}\,C\,m]$	74.5 ± 0.2	73.8 ± 0.2	78.6 ± 1.1

dioxane at the concentration of the EOA measurement, only the lowest energy vibronic band of the spectra were taken into account in the regression analysis. These bands originate from the nonaggregated monomer forms of the chromophores, while the higher energy bands strongly overlap with the dimer absorption. For the same reason, the absorption and EOA spectra of **1b** and **2b** are displayed in Figures S6 and S7 in the Supporting Information in relative units only. Compound **3a** did not show dimer formation in dioxane solution, providing

further evidence of its reduced dipolar nature relative to **1b** and **2b**. The spectra of **3a** are therefore displayed in conventional absolute units (Figure 3) and the regression could be extended over the complete CT band. The ground state dipole moments were calculated as usual[30] from $E - 6D$ (cf. Table 3) in the case of **3a** and from $E - 2D$ for **1b** and **2b**, taking contributions from electric field-induced dimer dissociation[22] into account. Dipole differences were calculated from the average values of regression coefficients F and G.[30]

Generally, the EOA spectra of the chromophores are governed by two effects. The first is the electrodichroic effect caused by orientation of the chromophores in the externally applied electric field. This effect is measured by the regression coefficient E. In all cases, strongly positive electrodichroism is observed: that is, the absorption for parallel polarization ($\phi = 0°$) of the incident light field relative to the externally applied field increases, while decreasing for the orthogonal polarization ($\phi = 90°$). This allows the conclusion that the ground state dipole moment μ_g and the transition dipole moment μ_{eg} are essentially parallel and oriented along the conjugated chain of the chromophores. The second effect is the band shift effect (Stark effect) of the CT band in the electric field due to the change in the dipole moment $\Delta\mu$ upon electronic excitation. The largest shift of the EOA spectrum relative to the optical absorption spectrum is clearly observed for **3a** (Figure 3), indicating a large value of $\Delta\mu$, while the shifts in the spectra of **1b** and **2b** (see Figures S6 and S7 in the Supporting Information) are much smaller.

Quantitative evaluation of the regression coefficients shows that the ground state dipole moment increases strongly in the sequence **3a**, **2b**, and **1b** (Table 3), while the dipole difference decreases and even becomes negative in the case of **1b**. This may be interpreted in terms of larger **ZW** contributions to the electronic ground states in **2b** and **1b**. The calculated resonance parameter c^2 shows that **1b** has the largest **ZW** character (56 %) and at the same time the largest ground state dipole moment. The **ZW** character of **2b** is considerably reduced (46 %), and **3b** is already largely **Q**-like (only 20 % **ZW** character). The resonance parameter c^2 correlates linearly with the ground state dipole moment, with slope 94×10^{-30} Cm and intercept at 14×10^{-30} Cm. The slope agrees reasonably with the value of $\Delta\mu_{max}$ and the intercept with the dipole moment of two cyano groups attached to a weakly polarized π system. Thanks to the close similarity of the topologies of the three chromophores, the dipole difference $\Delta\mu_{max}$ calculated in the CT model should be similar for all of them. In fact, the estimated values of $\Delta\mu_{max}$ are found to be almost identical for all chromophores, a result that nicely corroborates the model assumptions.

Ab initio computations

Need for computational approaches to provide a rationale for the experimental results and to assess predictability: The inversion of sign in the solvatochromic response on going from the pyridine and quinoline derivatives **1** and **2** to the acridine derivative **3** (Table 1), the large solvent-dependent ^{1}H NMR chemical shift variations of the pyridine-based system **1b** (Figure 2), and the dependence of the coupling

constant value of the central ethenylic unit on structural (pyridine–quinoline–acridine) and medium (dioxane–CHCl$_3$–DMSO) effects (Table 2) represent unequivocal experimental evidence of the high tuneability of the π-electron structure of the class of azinium-[-C≡C-thienyl]dicyanomethanido dyes **1**–**3**. Evidence that this result should be successfully translatable into structure- and medium-based fine control is suggested by the set of the β_0 experimental values obtained from EOA measurements in dioxane (Table 3) and by the very different NLO EFISH data obtained for system **1** when the solvent is shifted to CHCl$_3$ and DMF (Table 4).[7] Unfortunately, lack of NLO EFISH measurements for systems **2** and **3**, due to low solubility, and experimental difficulties in use of the EOAM technique in polar solvents, prevented us from obtaining a full set of experimental NLO values as a function of structure and solvent.

All these results are functions of the complex interplay of structural (BLA) and solvent effects. Experimentally based discrimination between the two contributions appears complex. We thus reverted to computational approaches and decided to perform a full and detailed ab initio investigation of the structural, electronic and NLO properties of systems **1**–**3**, considering both structural and solvent effects. Our goal is: a) to rationalize and complement available experimental data with a set of additional important parameters, b) to extend the investigation to media in which experimental measurements are not viable or reliable, including several solvents of different polarity and the gas phase. Agreement of experimental and computed results should, when both are available, allow us to produce a reliable picture of the effect of structure and medium on molecular properties, and conclusions based on the combination of different experimental techniques and ab initio study would be legitimate.

Computational details: Computational investigation was carried out for molecules **1c**–**3c**, taken as representative models of the compounds studied in this work, and on the assumption that the different substitution at the pyridine-like nitrogen (H versus Me, alkyl chain) would not affect the π-electron structure and NLO properties of the molecules. Results are therefore directly correlated with experimental data obtained for the species presented in the previous section. All ab initio computations used the GAUSSIAN 98[33]

program packages.[34] Because of the considerable size of the molecules under investigation and the high computational requirements due to the inclusion of the solvent effect (see below), we carried out full geometry optimizations and frequency computations at the Restricted Hartree–Fock (RHF) level of theory, using 6-31G* as a basis set and adopting C_s symmetry for all the species. Test density functional theory (DFT) calculations did not produce significantly different conclusions.[35] The higher computational cost and the belief that the accuracy of the HF approach would not be much improved by higher levels of theory for the purposes of our work discouraged us from pursuing different approaches. Conversely, for the reasons outlined in the previous section pertaining to the experimentally inaccessible full range of solvent polarities, we paid considerable attention to obtaining clues on the interaction of polarizable systems, such as **1**–**3**, with different media by means of calculations. Thus, structures, electronic parameters and β values were computed, taking the solvent effect into account by adoption of Onsager's self-consistent reaction field (SCRF) approach,[36] as available in the Gaussian package. In this model the chromophores are inserted in a spherical cavity in a continuum of solvent molecules: the solute radius and the dielectric constant ε of the solvent are the input parameters for Onsager SCRF computations.[37]

Ab initio ground state geometric and electronic computed parameters: To investigate the dependence of molecular parameters on solvent effects we have performed geometry optimization and charge computations with several solvent dielectric constants, ranging from 1.0 (gas phase) to 46.7 (DMSO). In this way, we were able to compute all the relevant molecular parameters in solvents of very different natures, going from apolar to highly polar media. However, for direct comparison with experimentally determined (NMR and β) data, most of the values presented refer to the gas phase and to the following solvents: dioxane ($\varepsilon = 2.21$), CHCl$_3$ ($\varepsilon = 4.80$), DMF ($\varepsilon = 36.70$), and DMSO ($\varepsilon = 46.70$).

Optimized structures of compounds **1c**–**3c** in the gas phase and in DMSO, dioxane and CHCl$_3$, including relevant bond length values, are presented in Figure 4, Figure 5, and Figures S8 and S9 (see the Supporting Information), respectively. Table S10 (in the Supporting Information) gives absolute energy values (atomic units) and frequency analysis

Table 4. Experimentally measured and computed[a] dipole moments and first hyperpolarizabilities of compounds **1**–**3**.

System (ε)		Gas phase			Dioxane[b] (2.2)			CHCl$_3$ (4.8)			DMF (36.7)		
		μ_g[c]	β_0[d]	$\mu\beta_0$[e]	μ_g[c]	β_0[d]	$\mu\beta_0$[e]	μ_g[c]	β_0[d]	$\mu\beta_0$[e]	μ_g[c]	β_0[d]	$\mu\beta_0$[e]
1	exptl				20.0	− 62	− 1240			− 6990[f]			− 2000[f]
	calcd [g]	18.4	17	310	27.1	− 30	− 810	45.8	− 210	− 9600	54.1	− 78	− 4200
		(20.3)			(28.2)			(37.5)			(50.8)		
2	exptl				16.9	44	750						
	calcd	16.6	22	360	24.2	31	750	47.6	− 230	− 11 000	56.9	− 69	− 3900
3	exptl				9.8	230	2230						
	calcd	14.3	29	420	19.8	89	1760	48.1	− 280	− 13500	58.5	− 62	− 3600

[a] RHF/6–31G*//RHF/6–31G*; C_s symmetry point group; compounds **1c**–**3c**. [b] Experimentally determined values from electrooptical absorption measurements on **1b**, **2b**, and **3a**. [c] in Debye. [d] Values according to the phenomenological convention (ref. [44]); 10^{-30} esu. [e] Values according to the phenomenological convention (ref. [44]); 10^{-48} esu. [f] EFISH measurements for compound **1c** (ref. [7]). [g] B3LYP/6–31G*//B3LYP/6–31G* computed values in parentheses.
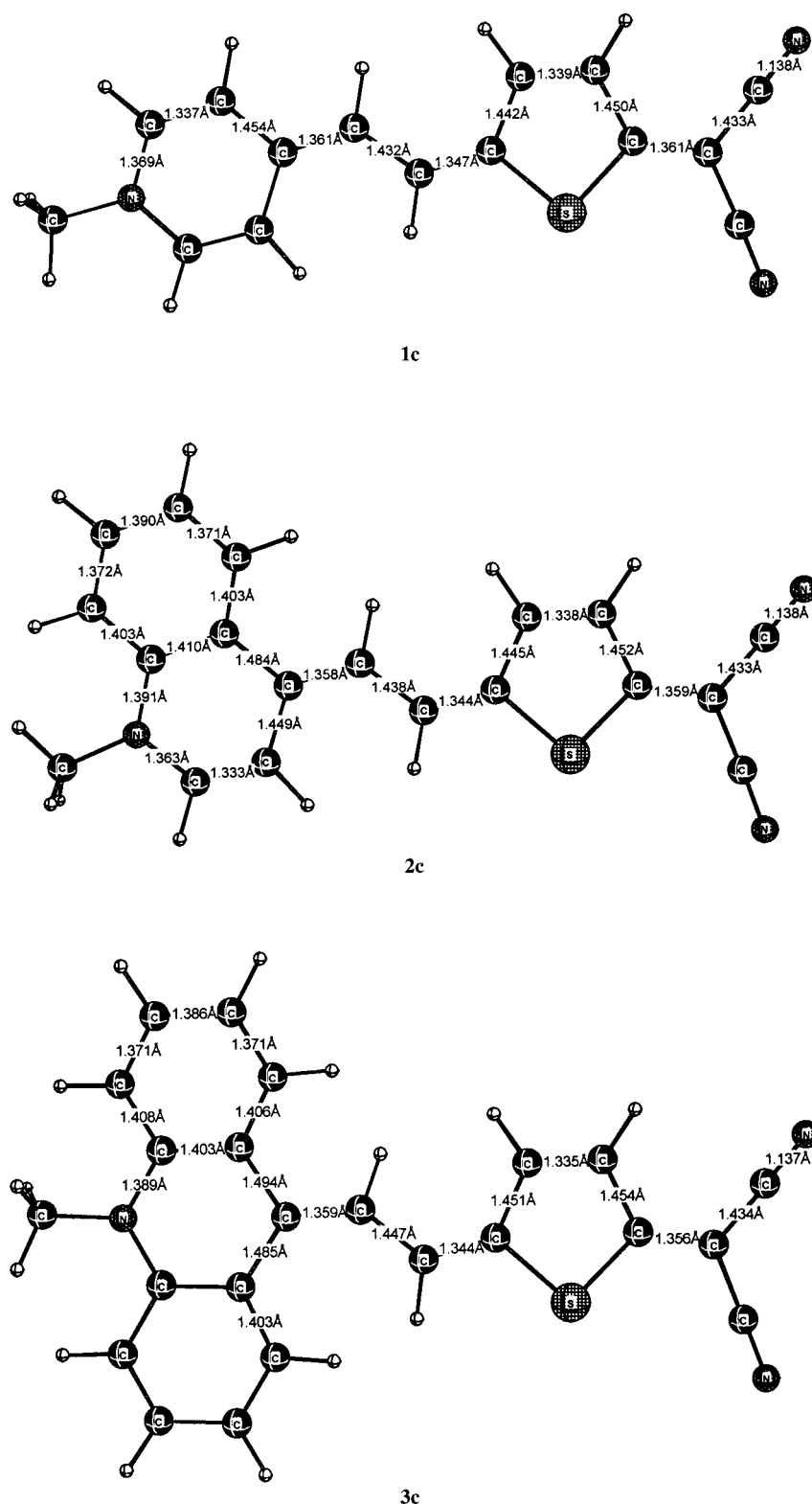
Figure 4. Optimized structures of chromophores **1c–3c** in the gas phase.

methyl rotation. In the case of **2c** and **3c**, frequency analysis therefore showed that the C_s geometry does not represent a local minimum. However, we have also assumed for these compounds that computational data relative to the C_s geometry would be sufficiently accurate for our purposes.[38]

The results clearly reveal not only that the structures of the three compounds are dramatically affected by the polarity of the surrounding media, but also that the predominant character (**ZW** versus **Q**) is not maintained throughout the range of polarity considered. In particular, the natures of the three systems are predominantly quinoid in the gas phase, whereas in the highly polar DMSO the zwitterionic character is strongly predominant. An intermediate situation is found for less polar solvents, such as dioxane and CHCl$_3$, in which, however, the contribution of the zwitterionic form is always predominant. Because of the benzocondensation of the azine ring on going from the pyridine to the quinoline and acridine derivative, the contribution of the quinoid limit form increases in all of the solvents on going from **1c** to **3c**.

A detailed quantitative investigation on the solvent-dependent ICT was performed by computation of natural charges (natural population analysis (NPA))[39, 40] in the gas phase and in different solvents, site by site (Figure 6). To focus attention better on acceptor–donor properties of the terminal moieties and on the extent of ICT, Figure 6 shows natural charges grouped by acceptor (azinium), donor (thienyldicyanomethanido), and bridging ethene units. In this way, we wanted quantitatively to probe the contribution of the two limit formulas to the description of the ground state in terms of natural charges residing on the two end groups. Namely, it was found that the negative total charge on the donor group (dicyanomethanido moiety) increases on going

results (number of imaginary frequencies) for the computed structures. Frequency analysis found one imaginary frequency for the pyridine derivative **1c**, corresponding to the *N*-methyl rotation. Two and three imaginary frequencies were found for the quinoline and acridine derivatives **2c** and **3c**, respectively. In both cases the lowest imaginary frequency is due to the

1c

2c

3c

Figure 5. Optimized structures of chromophores **1c**–**3c** in DMSO.

shared between the two side units, with no significant involvement of the central double bond, which remains substantially neutral.

The annelation effect, experienced on going from the pyridine **1c** to the quinoline **2c** and the acridine derivative **3c**, operates, in terms of charge distribution, in the direction of increasing quinoid character. Indeed, annelation promotes charge transfer from the donor to the acceptor site, as can be seen from the decrease in negative and positive total charge on the donor and acceptor moiety, respectively. A levelling off of annelation-induced charge variation is observed at higher polarities, as a consequence of a predominant *frozen* (less flexible) zwitterionic structure. These results are discussed, in conjunction with all other studies, in the following section.

Ab initio computed solvent-dependent first hyperpolarizabilities: Computed static (zero frequency) first hyperpolarizability β_0 values and $\mu\beta_0$ values are collected in Table 4 for a number of different media, together with experimentally ascertained values. Computed β_0 values were obtained at the HF level by the coupled perturbed Hartree–Fock (CPHF) method,[41] by use of the routine available in the Gaussian program. From the calculated values of the ten independent components β_{ijk} $(i,j,k = x,y,z)$ of the first hyperpolarizability tensor, we obtained β_{vec} and β_{tot} values from Equations (8)—(10),[42] through the adoption of Kleinman symmetry relations.[43]

from the poorly polar dioxane to the highly polar DMF and DMSO, consistently with an increased contribution of the **ZW** form in the latter two solvents. Total charges correspondingly became more positive on the acceptor group (azine moiety). It should be noted that the charge is almost symmetrically

$$\beta_i = \beta_{iii} + (1/3)\, \Sigma_{i \neq k}(\beta_{ikk} + \beta_{kik} + \beta_{kki}) \qquad i,k = x,y,z \qquad (8)$$

$$\beta_{vec} = (\mu_x\beta_x + \mu_y\beta_y + \mu_z\beta_z)/|\mu| \qquad (9)$$

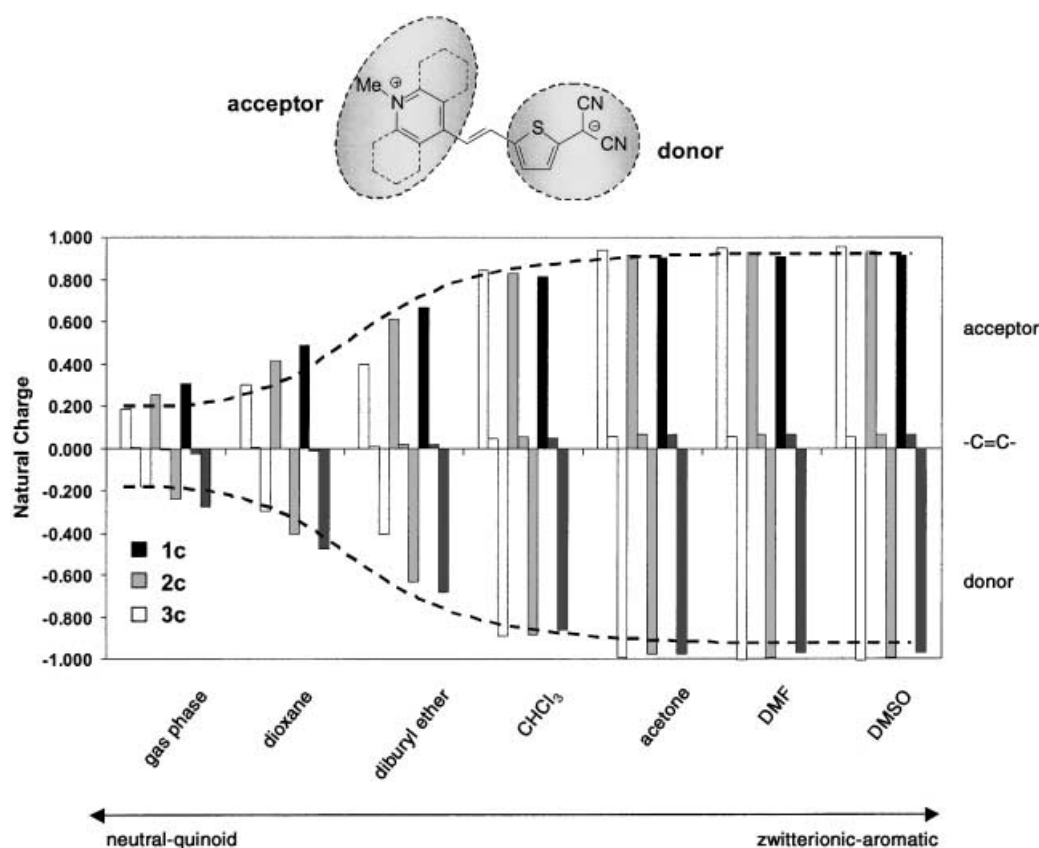$$\beta_{tot} = (\beta_x^2 + \beta_y^2 + \beta_z^2)^{1/2} \qquad (10)$$

Figure 6. Computed solvent-dependent natural charge distributions of compounds **1c – 3c**. Acceptor (left bar), ethenyl unit (mid bar), and donor (right bar) group charges are shown for each compound in each medium.

The β_{vec} values are identical to the β_{tot} values when the intramolecular charge transfer is collinear to the molecular ground-state dipole moment. We have checked that the two β values are very similar to each other and consequently only the β_{vec} values are presented. According to the "phenomenological" convention used in EFISH experimental measurements,[44] calculated β values were multiplied by a factor of 0.5 to make them directly comparable with experimentally determined values.

Discussion

Structural control of ICT: The extent of the solvatochromic response of these dyes in solution (Table 1) is the first indication of their high molecular polarizability. The $\Delta\lambda_{max}$ (DMSO → dioxane) sign inversion on going from the pyridine- to the acridine-based systems confirms the influence of molecular design at the acceptor level on fine control over the π-electron distribution on the whole chromophore structure. In this case we manipulate the aromaticity of the pyridinium/annelated pyridinium rings to control the π-electron-withdrawal strength of the end-heterocycle ring acceptor and therefore the extent of the charge transfer from the donor group. In fact, in the azine series (pyridine, quinoline and acridine)—as in the benzenoid one (benzene, naphthalene and anthracene)—the aromaticity of the central ring decreases through annelation. The result is a modulation of ground

state dipole moments, affecting optical[18] absorption in solution.

^{15}N and ^{13}C NMR experiments were performed in DMSO. Table 5 lists the sum of carbon chemical shifts on the ethenyl (C=C) and thienyldicyanomethanido (T(CN)$_2$) fragments and in the whole donor-spacer unit (Tot.). Chemical shifts can be converted into π-electron densities (Δq^π) on the carbon framework by use of Equation (1). Values are reported as variations with respect to the system **1**, taken as a reference. Note that only the donor-spacer fragment was considered in this computation, since it remains unchanged along the whole series of chromophores. Therefore, on moving from the pyridine-based systems **1a/b** to the corresponding quinoline **2a/b** and acridine **3a** derivatives, total q^π variations (Δq^π Tot) can be ascribed only to intramolecular charge transfer

Table 5. Sum ($\Sigma\delta$) of the ^{13}C shifts [ppm] of **1 – 3** on the ethenyl (C=C) and thienyldicyanomethanido (T(CN)$_2$) molecular fragments and variation of the local π-electron densities Δq^π on going from **1a/b** to the corresponding **2a/b** and **3a** systems.

Compound	$\Sigma\delta$(^{13}C NMR)			$\Delta q^{\pi[a]}$		
	C=C	T(CN)$_2$	Tot	C=C	T(CN)$_2$	Tot
1a	247.9	814.7	1062.6	0.00	0.00	0.00
1b	247.3	816.4	1078.7	0.00	0.00	0.00
2a	244.4	834.3	1063.7	0.02	− 0.12	− 0.10
2b	244.0	835.1	1079.1	0.02	− 0.12	− 0.10
3a	252.9	834.3	1087.1	− 0.03	− 0.12	− 0.15

[a] Calculated according to Equation (1); negative values correspond to a decrease of π-electron density

promoted by pyridine annelation. From this study two important conclusions can be drawn. First, *N*-protonated (**a** derivatives) and *N*-alkylated (**b** derivatives) systems exhibit identical Δq^{π} values (**1a** → **2a** and **1b** → **2b**). Thus, π-molecular polarization is substantially independent of H/alkyl σ substitution at the azine nitrogen atom and makes it legitimate to compare the NLO properties of differently σ-functionalized derivatives at the azine nitrogen. Second, on going from the pyridine to the quinoline and then to the acridine dye there is a slight decrease (−0.10 and −0.15, respectively) in the π-electron density on the donor site. This experimental evidence is nicely in accord with the greater accepting properties of acridinium and quinolinium relative to the pyridinium group. In addition, this result is even more important in view of the fact that DMSO is certainly not the best solvent in which to evaluate this trend, since its high polarity pushes all the three chromophores toward their zwitterionic limit. Under such conditions, the π-framework along the ICT direction is almost identical in all of the chromophores, and so the charge distribution on the donor site is similar in the three species. Unfortunately, poor chromophore solubility in solvents of low dielectric constant, in which higher overall sensitivities would be expected, prevented us from performing multinuclear NMR experiments in CHCl$_3$ and dioxane.

The above behavior is in full agreement with the predications of ab initio computation. From the computed absolute π-electron densities in DMSO, it is possible to derive the Δq^{π} values for the -(C=C)-thienyldicyanomethanido fragment, if molecule **1c** is taken as the reference system. The computed Δq^{π} values are indeed very small ($\Delta q^{\pi} < 0.004$ electrons) and differences in the three systems are negligible. In short, the high solvent polarity of DMSO freezes the chromophore π-electron distribution in an almost completely charge-separated (**ZW**) structure.

Environmental control of ICT: Medium polarity proves to be a very efficient tool with which to steer the molecular response for highly polarizable systems such as

those presented here. Both ^{13}C NMR and computation have shown the *rigidity* of the π-structure in highly polar solvents such as DMSO. However, things change dramatically when solvent polarity starts to decrease. A first hint of this behavior is the drastic change in the ^{1}H NMR chemical shifts and H-C≡C-H coupling constants in **1–3** as a function of solvent polarity.

An interesting complementary way to visualize the strongly solvent-dependent molecular properties is to plot the computed ground state dipole moment μ values against the solvent's dielectric constant ε (Figure 7a). Two regions of ε
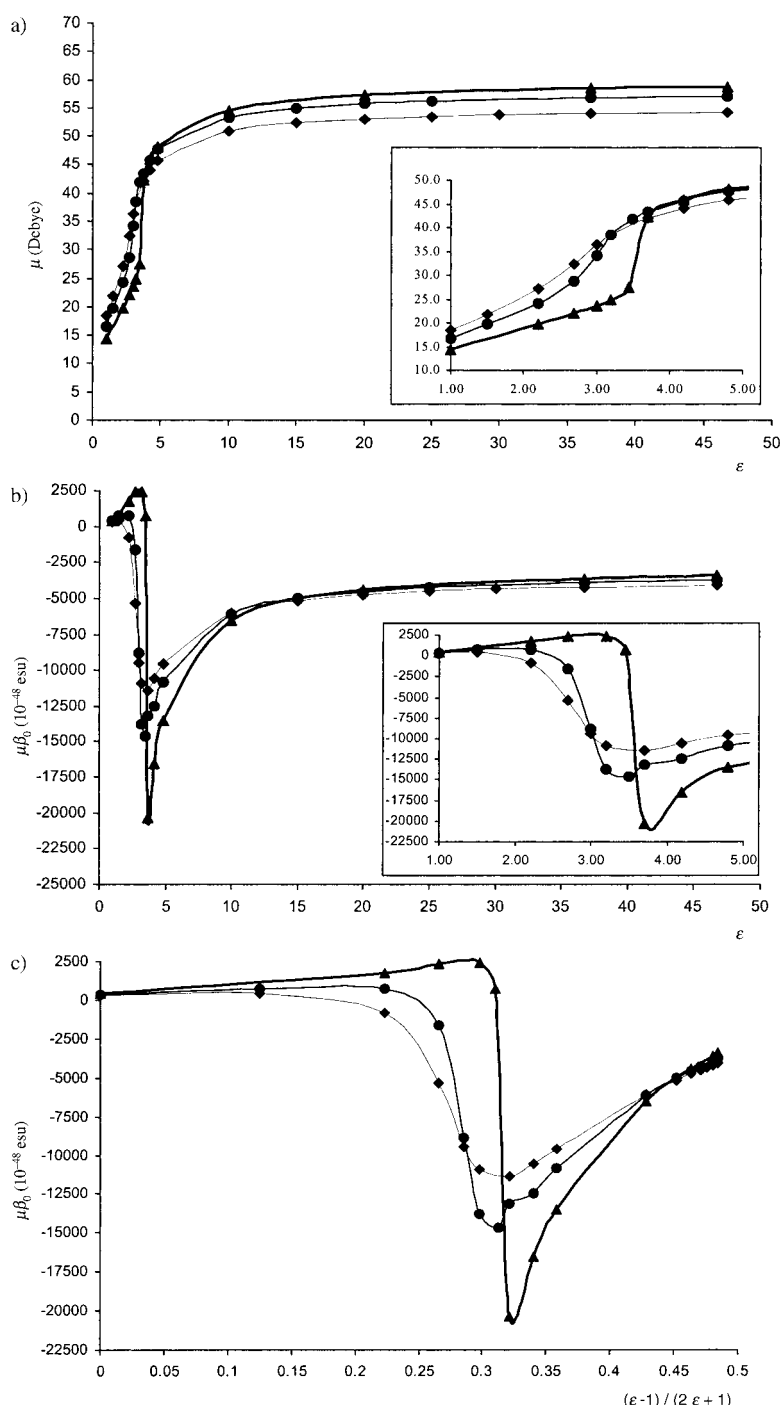

Figure 7. Plots of computed μ (a) and static $\mu\beta_0$ (b) against dielectric constant ε of the surrounding medium, and $\mu\beta_0$ against $(\varepsilon - 1)/(2\varepsilon+1)$ (c) for **1c** (♦), **2c** (●), and **3c** (▲).

values with different effects are then identified: 1) a large range ($7 < \varepsilon < 47$) of dielectric constants in which μ values of chromophores **1–3** are very large and do not vary significantly either with structure or with solvent polarity; this is in agreement with predominantly zwitterionic character in the systems, and 2) a much smaller ε range ($1 < \varepsilon < 7$) in which the dipole moments decrease dramatically; here the contribution of the quinoid structure increases for all the systems, in particular for the acridine-based derivative **3a**.

This very large sensitivity of the π-structure in the $1 < \varepsilon < 7$ range is confirmed by the solvatochromic response of **1b** in bulk. Host–guest films of **1b** were prepared with matrices of different dielectric constants. Loading of **1b** was kept very low (< 0.5 wt%) to prevent formation of aggregates and microdomains and to avoid substantial changes in ε on going from the pure matrix to the blend. In particular, we chose host polymer matrices with low dielectric constants, to match the region in which the molecular polarization of dyes **1–3** is significantly affected. Some of these templates—such as PMMA, polyimides, and sol–gel glasses—have been extensively used in the preparation of active electrooptic materials.[45] The solid-state solvatochromic data for **1b** are collected in Table 6. The solvatochromic shift of dye **1b** from the low-polar polystyrene ($\varepsilon = 2.5–2.6$; Table 6, entry 8) to the high-polar siliceous matrix ($\varepsilon > 6$; entry 1) is extremely large ($\Delta\lambda_{max}$ as high as -132 nm). This surprisingly high solvatochromic shift, even larger than that found in solution ($\Delta\lambda_{max} = -89$ nm), is probably due to the peculiar nature of the siliceous matrix, in which multiple and strong intermolecular interactions occur between the highly polar dye and the pore surface, exposing hydroxy functionalities.[46]

Table 6. Solvatochromic data (λ_{max} [nm] of the charge-transfer band) for the chromophore **1b** in selected film matrices.

Entry	Matrix	ε	λ_{max} [nm]
1	siliceous	> 6	592
2	poly(p-hydroxystyrene)	[a]	616
3	poly(ethyleneglycol)	3.6–4.0	628
4	**1b**[b]	[a]	648
5	PMMA	3.2–3.5	676
6	polymaleimide	3.1–3.3	680
7	poly(vinylbenzyl chloride)	2.7–2.9	702
8	polystyrene	2.5–2.6	724

[a] Unknown. [b] As free standing neat film obtained by spin coating.

Finally, Table 7 shows computed ethenyl bond lengths of the central spacer unit in dioxane, chloroform, and DMSO for compounds **1–3**. A progressive elongation of this bond in the series of chromophores is observed when the solvent polarity is concomitantly increased. This data demonstrate the varia-

Table 7. Solvent-dependent computed C–C bond lengths [Å] of the central ethenylic unit in systems **1–3**.[a]

Compound	Dioxane	CHCl₃	DMSO
1c	1.404	1.348	1.337
2c	1.417	1.347	1.337
3c	1.435	1.349	1.340

[a] Calculated at the RHF/6–31G*//RHF/6–31G* level; C_s symmetry point group.

ble contribution of the **Q** and **ZW** limit formulas to dyes' descriptions, with an increased/decreased contribution of the **ZW/Q** structure in higher polar solvents. This result is fully supported experimentally by the ^3J behavior of this bond in such solvents.

Nonlinear optical molecular response: Table 4 collects both experimentally determined (EFISH and EOAM) and computed μ, β_0 and $\mu\beta_0$ values for **1–3** in different media. The excellent agreement found between the computed and the available experimental $\mu\beta_0$ results, also taking account of the implicit errors arising from measurements and computational approximations, is remarkable and allow us to view the computed values in solvents for which NLO experimental data are not accessible as realistic.

The overall picture that emerges from the combination of experimentally determined and computational investigation leads to important and, in some ways, amazing and unexpected conclusions.

First, chromophore NLO β_0 responses are low and positive in media of very low dielectric constant (gas phase) while being low and negative in solvents of high dielectric constant (DMF). Note that $\mu\beta_0$ (DMF) is indeed much higher than $\mu\beta_0$ (gas) but that most of the contribution comes from the higher μ values. Indeed, these results are to be expected because both limit situations are characterized by a molecular π-structure *frozen* in either the quinoid or the zwitterionic limit formula. In accordance with the two-state model, these situations lead to the lowest second-order NLO activity. In this context (at these extreme situations) annelation of the pyridine acceptor has very little influence on the extent of the charge transfer and the molecular properties are environmentally controlled. These data are in line with the solvatochromic and NMR results.

Second, completely different behavior is observed when media possessing suitable dielectric constants ($2 < \varepsilon < 7$), such as chloroform and dioxane solvents, are considered. We have already shown how they greatly affect the molecular dipole moments. In this case the description of the dyes' ground or excited states is a "*loose*" combination of both Q and ZW limit formulas, which can easily be perturbed. In this situation, slight structural modifications and/or minute ε variations greatly affect the nonlinear optical response. In dioxane, simply through annelation of the pyridine ring, $\mu\beta_0$ changes from negative (ca. -1200 for **1b**) to positive (ca. $+800$ for **2b**) to highly positive (ca. $+2200$ for **3a**). Moving from dioxane to chloroform ($\Delta\varepsilon \approx 2.6$) the nonlinear optical figure of merit $\mu\beta_0$ increases by a factor of ten. However, to stress the overall sensitivity of **1–3** second-order NLO responses with medium polarity, Figure 7b and Figure S11 (in the Supporting Information) show plots of $\mu\beta_0$ and β_0, respectively, against ε. Alternatively, the permittivity dependence of $\mu\beta_0$ in terms of the function $(\varepsilon - 1)/(2\varepsilon + 1)$, which controls the magnitude of the reaction field,[8d] is illustrated in Figure 7c.

These graphs clearly show the highly strategic role of the polarity of the surrounding media in determining the NLO molecular response. It should be noted how, upon changing the value of the dielectric constant ε, $\mu\beta_0$ values can not only change sign, but more importantly, vary by orders of

magnitude. For instance, $|\mu\beta_0|$ of acridine derivatives is predicted to change from zero to 2.2×10^{-44} esu (a value that would be one of the largest ever reported in the literature) within a range of only 0.4 ε units (from 3.4 to 3.8)!

Conclusion

In this study a combination of organic synthesis, multinuclear (^{1}H, ^{13}C, ^{15}N) NMR study, optical absorption spectroscopy, nonlinear optical measurements, and ab initio computations have been applied to the design, preparation, and characterization of a novel family of push–pull chromophores **1—3**, in which fine control over molecular properties is based on structural and media effects.

The chromophore design of the electron-poor central pyridine ring as a π-acceptor unit conjugated with the dicyanomethanido donor, based on the different aromaticity achieved through annelation, provides a set of structures that exhibits either similar or differentiated properties, depending on the surrounding media. In fact, the ground and excited states of these systems can be described as linear combinations of two limit formulas, **ZW** and **Q**, the relative weights of which significantly affect the molecular performance in terms of linear and nonlinear optical responses.

This study demonstrates that dyes **1–3** are undoubtedly highly polarizable structures. On the basis of multinuclear NMR analysis and solvatochromic data, all of the systems **1–3** are primarily zwitterionic over a large range of high dielectric constants, while the quinoid contribution increases as ε decreases. Eventually, they are completely quinoid for $\varepsilon < 2$. These results are confirmed both by nonlinear optical measurements in dioxane, chloroform and DMF and by computations. Bond-localized quinoid arrangements must be a realistic structural prerequisite: their evolution into charge-separated structures by ICT must be made possible by favorable interaction with polar media. Computations are invaluable in suggesting proper environments for adjusting the ICT and should allow improvement, even of orders of magnitude, of the first hyperpolarizability performance of highly polarizable NLO-phores.

In short, dyes **1–3** give access to large second-order molecular NLO activities, which can only be reached, however, if medium polarity effects are carefully taken into consideration. An excellent NLO response in solution might vanish when the active chromophore is dispersed in a matrix with unsuitable dielectric properties. Vice versa, a mediocre NLO response for a newly designed chromophore could be the result of an unfortunate choice of solvent, as dictated by instrumental availability or solubility properties; the same chromophore might prove to perform very well under appropriately chosen environmental (solvent, matrix) conditions. The commonly established procedure for NLO compounds to report β values in one solvent only, may in certain cases be insufficient to draw definite conclusions on the overall chromophore performance and the prospect of different design strategies.

Experimental Section

General: ^{1}H NMR spectra were recorded at 300 and 500 MHz. UV/Vis spectra were recorded with a Varian Cary 1 E spectrophotometer. Mass spectra were determined at an ionizing voltage of 70 eV. Anhydrous solvents were prepared by continuous distillation over sodium sand, in the presence of benzophenone and under nitrogen or argon, until the blue color of sodium ketyl was permanent. Anhydrous *N,N*-dimethylformamide (DMF) was supplied by Fluka. Acetone was dried over Na_2SO_4 for a few days. Diisopropylamine was heated at reflux over CaH_2 for 4 h and distilled under nitrogen prior to use. Extracts were dried over Na_2SO_4 (4 h). Melting points are uncorrected.

Electrooptical absorption measurements (EOAM): The EOAM characterization of the NLO-phores was carried out by previously described methods.[16, 31] Electrooptical absorption spectra were recorded in dioxane, which was purified and carefully dried prior to use by distillation from Na/K under argon. Supplementary optical absorption spectra required for evaluation of the EOAM spectra were determined with a Perkin-Elmer Lambda 900 spectrophotometer.

Materials: 4-Pyridinecarbaldehyde, 4-quinolinecarbaldehyde, and 2-bromothiophene were commercially available. 1-(4-Pyridyl)-2-{2-[5-(dicyanomethanido)thienyl]}ethene sodium salt and decyl triflate were prepared by known procedures.[6]

Film preparation: A solution of **1b** (0.1 mg) in THF (0.1 mL) was added to a solution obtained from polymeric samples (entries 2, 3, 5--8, Table 6, ≈15 mg) dissolved by sonication in either THF or $CHCl_3$ (1 mL). The mixture was sonicated for 2 min and then spin-coated (1500–2000 rpm, 10 s) onto sodium lime glass substrates (Fisher). A **1b** film (entry 4, Table 6) was prepared by spin-coating a solution of **1b** (5 mg) in $CHCl_3$ (1 mL). Siliceous film (entry 1, Table 6) was prepared from a mixture of **1b** (0.2 mg) and $Si_3O_3Cl_8$ (0.01 mL) in THF (1 mL). After spin-coating, the film was dried under vacuum for 10 min and rinsed twice with diluted ammonium hydroxide solution (2%) and finally with water. UV/Vis spectra were immediately recorded after film preparation.

1-(4-1*H*-Pyridinium)-2-[2-[5-(dicyanomethanido)thienyl]}ethene (1a): Aqueous HCl (10%) was added dropwise to a suspension of 1-(4-pyridyl)-2-{2-[5-(dicyanomethanido)thienyl]}ethene sodium salt (0.185 g, 0.68 mmol) in H_2O (5 mL) until pH 1 was reached. After the mixture had been stirred at room temperature for 30 min, the blue precipitate was collected, washed with water, and dried under vacuum at 80 °C to afford the pure product (0.140 g, 0.56 mmol, 82.4%): m.p. 234–235 °C(DMF); ^{1}H NMR ([D$_6$]DMSO, 25 °C, TMS): $\delta = 14.2$ (broad, 1H), 8.40 (d, ^3J(H,H) = 7.0 Hz, 2H), 7.97 (d, ^3J(H,H) = 15.1 Hz, 1H), 7.75 (d, 2H), 7.19 (d, ^3J(H,H) = 4.2 Hz, 1H), 6.34 (d, 1H), 6.25 (d, 1H); elemental analysis calcd (%) for $C_{14}H_9N_3S \cdot 0.5 H_2O$ (260.3): C 64.58, H 3.87, N 16.14; found: C 65.01, H 4.02, N 15.61.

1-(4-1-Decylpyridinium)-2-[2-[5-(dicyanomethanido)thienyl]ethene (1b): Decyl triflate (0.21 g, 0.74 mmol) in dry acetone (1 mL) was added dropwise to a suspension of 1-(4-pyridyl)-2-{2-[5-(dicyanomethanido)thienyl]}ethene sodium salt (0.19 g, 0.70 mmol) in the same solvent (4 mL). The color of the solution changed immediately from orange to blue. After the mixture had been stirred overnight at room temperature, the precipitate was collected and washed with EtOH and water to give the practically pure product (0.141 g, 0.36 mmol, 51.4%) as a blue solid: m.p. 225–226 °C (EtOH); ^{1}H NMR ([D$_6$]DMSO, 25 °C, TMS): $\delta = 8.45$ (d, ^3J(H,H) = 7.1 Hz, 2H), 7.99 (d, ^3J(H,H) = 15.1 Hz, 1H), 7.75 (d, 2H), 7.20 (d, ^3J(H,H) = 4.2, 1H), 6.35 (d, 1H), 6.25 (d, 1H), 4.25 (t, ^3J(H,H) = 7.2 Hz, 2H), 1.81 (m, 2H), 1.18–1.35 (m, 14H), 0.84 ppm (t, ^3J(H,H) = 6.9 Hz, 3H); elemental analysis calcd (%) for $C_{24}H_{29}N_3S \cdot 0.5 H_2O$ (400.6): C 71.95, H 7.56, N 10.49; found: C 71.95, H 7.16, N 10.07.

1-(4-1*H*-Quinolinium)-2-[2-[5-(dicyanomethanido)thienyl]ethene (2a): Aqueous HCl (10%) was added dropwise to a suspension of 1-(4-quinolyl)-2-{2-[5-(dicyanomethanido)thienyl]}ethene sodium salt (0.21 g, 0.645 mmol) in H_2O (7 mL) until pH 1 was reached. After the mixture had been stirred for 30 min at room temperature, the blue precipitate was collected, washed with water and dried under vacuum to afford the pure product (0.16 g, 0.52 mmol, 82.3%): m.p. >240 °C; ^{1}H NMR ([D$_6$]DMSO, 25 °C, TMS): $\delta = 14.10$ (s, 1H), 8.62 (d, ^3J(H,H) = 8.6 Hz, 1H), 8.51 (d, ^3J(H,H) = 6.5 Hz, 1H), 8.26 (d, ^3J(H,H) = 14.3 Hz, 1H), 7.93 (t, ^3J(H,H) =

7.8 Hz, 1H), 7.86 (d, ^3J(H,H) = 8.4 Hz, 1H), 7.81 (d, 1H), 7.68 (t, 1H), 7.46 (d, ^3J(H,H) = 4.2 Hz, 1H), 6.99 (d, 1H), 6.45 ppm (d, 1H); elemental analysis calcd (%) for $C_{18}H_{11}N_3S \cdot 2H_2O$ (337.4): C 64.07, H 4.49, N 12.45; found: C 64.41, H 4.27, N 12.88.

1-(4-1-Decylquinolinium)-2-{2-[5-(dicyanomethanido)thienyl]}ethene (2b): Decyl triflate (0.49 g, 1.71 mmol) in dry acetonitrile (30 mL) was added dropwise to a suspension of 1-(4-quinolyl)-2-{2-[5-(dicyanomethanido)thienyl]}ethene sodium salt (0.50 g, 1.55 mmol) and K_2CO_3 (0.64 g, 4.65 mmol) in the same solvent (30 mL). The color of the solution changed immediately from orange to green. After the mixture had been heated at reflux for 2 h, the solvent was evaporated and the residue was chromatographed on alumina (neutral, acetone/CHCl₃ 1:1) to afford the pure product (0.09 g, 0.20 mmol, 13.1%): m.p. 156–158°C; ^{1}H NMR ([D₆]DMSO, 25°C, TMS): δ = 8.69 (d, ^3J(H,H) = 8.8 Hz, 1H), 8.55 (d, ^3J(H,H) = 7.05 Hz, 1H), 8.29 (d, ^3J(H,H) = 14.2 Hz, 1H), 8.11 (d, 1H), 7.98 (t, ^3J(H,H) = 7.4 Hz, 1H), 7.77 (d, 1H), 7.70 (t, 1H), 7.49 (d, ^3J(H,H) = 4.3 Hz, 1H), 7.01 (d, 1H), 6.50 (d, 1H), 4.57 (t, ^3J(H,H) = 7.22, 1H), 1.82 (m, 2H), 1.40–1.10 (m, 14H), 0.84 ppm (t, J(H,H) = 6.5, 3H); elemental analysis calcd (%) for $C_{28}H_{31}N_3S$ (441.7): C 76.27, H 7.50, N 9.20; found: C 76.18, H 6.98, N 9.38.

1-(4-Quinolyl)-2-[5-(dicyanomethanido)thien-2-yl]ethene sodium salt (5): Malononitrile (0.35 g, 5.30 mmol) was added portionwise to an ice-cooled suspension of sodium hydride (0.25 g, 60% in oil, 6.25 mmol) in anhydrous 1,2-dimethoxyethane (27 mL), and the mixture was stirred under nitrogen atmosphere at room temperature for 30 min. 1-(4-Quinolyl)-2-(5-bromothien-2-yl)ethene (0.64 g, 2.22 mmol) and tetrakis(triphenylphosphine)palladium(0) (0.25 g, 0.22 mmol) were added to the above solution, and the mixture was stirred overnight at room temperature. The solvent was removed under reduced pressure and the resulting gummy solid was taken up with benzene (3 × 10 mL) and hexane (30 mL), and finally washed with H_2O (2 × 8 mL) to give the product as a red-brown solid (0.67 g, 2.07 mmol, 93.2%), which was used in the next step without further purification: m.p. >240°C; ^{1}H NMR ([D₆]DMSO, 25°C, TMS): δ = 8.72 (d, ^3J(H,H) = 4.8 Hz, 1H), 8.33 (d, ^3J(H,H) = 8.3 Hz, 1H), 7.95 (d, ^3J(H,H) = 8.5 Hz, 1H), 7.72 (t, 1H), 7.68 (d, 1H), 7.66 (d, ^3J(H,H) = 11.8 Hz, 1H), 7.57 (t, 1H), 7.04 (d, 1H), 7.03 (d, 1H), 6.09 ppm (d, ^3J(H,H) = 3.8 Hz, 1H).

1-(4-Quinolyl)-2-(5-bromothien-2-yl)ethene (7): A mixture of 5-bromo-2-chloromethylthiophene[47] (4.60 g, 21.76 mmol) and triethylphosphite (3.60 g, 21.76 mmol) was heated at reflux at 110°C for 6 h. The resulting oil was heated at 200°C and at 1 mmHg in a Kugelrohr apparatus to distil low-boiling components, leaving the diethyl 5-bromothien-2-ylmethanephosphonate (6.02 g, 19.22 mmol, 88%) as a light red, oily residue; this was used for subsequent steps without further purification. ^{1}H NMR (CDCl₃, 25°C, TMS): δ = 6.88 (d, ^3J(H,H) = 3.7 Hz, 1H), 6.71 (tt, ^4J(P,H) = 1.0 Hz, ^3J(H,H) = 3.7 Hz, 1H), 4.07 (dq, ^3J(P,H) = 8.22 Hz, 6H), 3.26 (dd, ^2J(P,H) = 20.7 Hz, 2H), 1.28 ppm (t, ^3J(H,H) = 7.1 Hz, 9H).

A suspension of sodium hydride in oil (60% by weight; 0.16 g, corresponding to 0.27 g, 6.96 mmol) was thoroughly washed with anhydrous hexane and then suspended in anhydrous THF (15 mL). A solution of diethyl 5-bromothien-2-ylmethanephosphonate (1.99 g, 6.36 mmol) in THF (5 mL) was added under nitrogen to this suspension, followed by the addition of a solution of 4-quinolylcarbaldehyde (1.00 g, 6.36 mmol) in the same solvent (5 mL). The mixture was cautiously heated on an oil-bath at 50°C until the evolution of hydrogen had ceased, and then at reflux for 2 h. The mixture was poured onto ice (100 mL) and the aqueous phase was extracted with ether (4 × 50 mL). The ethereal phases were combined, washed with water and dried over Na_2SO_4, and the solvent was finally evaporated to afford a dark oil (1.97 g). The pure product was obtained after column chromatography (silica gel, ether) as a light yellow solid (1.041 g, 3.29 mmol, 51.7%): m.p. 113–114°C (after sublimation); ^{1}H NMR ([D₆]DMSO, 25°C, TMS): δ = 8.87 (d, ^3J(H,H) = 4.7 Hz, 1H), 8.42 (d, ^3J(H,H) = 7.9 Hz, 1H), 8.03 (d, ^3J(H,H) = 7.9 Hz, 1H), 7.81 (d, 1H), 7.79 (t, ^3J(H,H) = 6.9 Hz, 1H), 7.73 (s, 2H), 7.66 (t, 1H), 7.32 (d, ^3J(H,H) = 3.8 Hz, 1H), 7.28 (d, 1H); elemental analysis calcd (%) for $C_{15}H_{10}BrNS$ (316.2): C 56.98, H 3.19, N 4.43; found: C 57.31, H 3.42, N.4.67

1-(4-10H-Acridinium)-2-{2-[5-(dicyanomethanido)thienyl]}ethene (3a): Aqueous HCl (10%) was added dropwise to a suspension of 1-(9-acridyl)-2-{2-[5-(dicyanomethanido)thienyl]}ethene sodium salt (1.91 g,

5.10 mmol) in H_2O (50 mL) until pH 1 was reached. After the mixture had been stirred at room temperature for 30 min, the blue precipitate was collected, washed with water, and dried under vacuum at 80°C to afford the pure product (1.49 g, 4.22 mmol, 82.9%). m.p. >300°C(DMF); ^{1}H NMR ([D₆]DMSO, 25°C, TMS): δ = 12.2 (broad, 1H), 8.27 (d, ^3J(H,H) = 8.3 Hz, 2H), 8.01 (d, ^3J(H,H) = 13.5 Hz, 1H), 7.84 (d, ^3J(H,H) = 4.9 Hz, 1H), 7.71 (t, ^3J(H,H) = 7.6 Hz, 2H), 7.52 (d, ^3J(H,H) = 8.2 Hz, 2H), 7.35 (t, ^3J(H,H) = 7.6 Hz, 2H), 7.16 (d, ^3J(H,H) = 13.7 Hz, 1H), 6.88 ppm (d, ^3J(H,H) = 4.9 Hz, 1H); elemental analysis calcd (%) for $C_{22}H_{13}N_3S$ (351.4): C 75.19, H 3.73, N 11.96, S 9.12; found: C 75.03, H 3.81, N 11.51, S 8.60.

1-(9-Acridyl)-2-{2-[5-(dicyanomethanido)thienyl]}ethene sodium salt (6): A solution of malononitrile (0.15 g, 2.2 mmol) in 1,2-dimethoxyethane (4 mL) was added to an ice-cooled suspension of sodium hydride (0,18 g, 60% in mineral oil, 4.5 mmol) in the same solvent (10 mL), and the mixture was stirred at room temperature under nitrogen for 1 h. 1-(9-Acridyl)-2-(5-bromothien-2-yl)ethene (0.41 g, 1.1 mmol) and tetrakis(triphenylphosphine)palladium(0) (0.14 g, 0.1 mmol) were added, and the reaction mixture was stirred overnight at room temperature. The solvent was remove under reduced pressure, and the solid was taken up with dry benzene (25 mL) and washed with water (5 mL) to give the product as a purple solid (0.41 g; 1.1 mmol; 97%). m.p. >240°C; ^{1}H NMR ([D₆]DMSO, 25°C, TMS): δ = 8.39 (d, ^3J(H,H) = 8.7 Hz, 2H), 8.09 (d, ^3J(H,H) = 8.6 Hz, 2H), 7.81 (t, ^3J(H,H) = 7.6 Hz, 2H), 7.58 (t, ^3J(H,H) = 7.7 Hz, 2H), 7.26 (s, 2H), 7.03 (d, ^3J(H,H) = 3.9 Hz, 1H), 6.10 ppm (d, ^3J(H,H) = 3.9 Hz, 1H).

1-(9-Acridyl)-2-(5-bromothien-2-yl)ethene (8): A mixture of sodium acetate (8.17 g, 99.6 mmol), acetic acid (98%, 28 mL), and 9-methylacridine (1.63 g, 8.5 mmol) was heated at 80°C for few minutes. 5-Bromo-2-thiophenecarbaldehyde (3.22 g, 17.0 mmol) was then added, and the reaction mixture was heated at reflux for 8 h. After cooling, the reaction mixture was poured into iced water (140 mL), and ammonium hydroxide (25%) was added until pH 14 was reached. The basic solution was extracted with ethyl acetate (5 × 65 mL) and the organic phase was washed twice with water and dried over Na_2SO_4, and the solvent was evaporated to give the crude product (4.05 g), which was purified by column chromatography on silica gel (dichloromethane/diethyl ether 20:1). Two isomers were isolated: *cis* isomer (0.21 g, 0.6 mmol, 6.6%): m.p. 134–135°C; ^{1}H NMR (CDCl₃, 25°C, TMS): δ = 8.28 (d, ^3J(H,H) = 8.8 Hz, 2H), 8.15 (d, ^3J(H,H) = 8.6 Hz, 2H), 7.76–7.82 (m, 2H), 7.45–7.53 (m, 2H), 7.28 (d, ^3J(H,H) = 12.1 Hz, 1H), 6.99 (d, ^3J(H,H) = 12.1 Hz, 1H), 6.70 (d, ^3J(H,H) = 3.9 Hz, 1H), 6.64 ppm (d, ^3J(H,H) = 3.9 Hz, 1H); MS (EI, 70 eV): m/z (%): 367 (52) $[M]^+$; *trans* isomer (1.10 g, 3.0 mmol, 35.5%): m.p. 197–200°C (AcOEt); ^{1}H NMR (CDCl₃, 25°C, TMS) δ = 8.27 (d, ^3J(H,H) = 8.8 Hz, 2H), 8.24 (d, ^3J(H,H) = 8.7 Hz, 2H), 7.74–7.82 (m, 2H), 7.63 (d, ^3J(H,H) = 16.3 Hz, 1H), 7.51–7.58 (m, 2H), 7.07 (d, ^3J(H,H) = 16.3 Hz, 1H), 7.05 (d, ^3J(H,H) = 3.9 Hz, 1H), 6.94 ppm (d, ^3J(H,H) = 3.9 Hz, 1H); MS (EI, 70 eV): m/z (%): 367 (100) $[M]^+$; elemental analysis calcd (%) for $C_{19}H_{12}BrNS$ (366.3): C 62.30, H 3.30, N 3.82; found: C 61.80, H 3.26, N 3.69.

9-Methylacridine (9): A mixture of diphenylamine (13.25 g, 78.3 mmol), acetic acid (60%, 8 mL), and $ZnCl_2$ (22.91 g, 168.1 mmol) was heated at 170°C for 17 h. After cooling, the solid was taken up with warm water (2 × 50 mL), which was discarded, and then extracted with hot water (4 × 60 mL). The aqueous phases were combined, NH_4OH (30%) was added, and the basic solution was extracted with ethyl acetate (3 × 200 mL). The organic phase was washed with water (100 mL) and dried over Na_2SO_4, and the solvent was evaporated to give the product as a yellow solid (4.01 g, 20.8 mmol, 26.5%). m.p. 114°C (lit.[48] 114–115°C); ^{1}H NMR (CDCl₃, 25°C, TMS): δ = 8.22 (d, ^3J(H,H) = 8.8 Hz, 2H), 8.19 (d, ^3J(H,H) = 8.6 Hz, 2H), 7.71 (t, ^3J(H,H) = 7.4 Hz, 2H), 7.50 (t, ^3J(H,H) = 7.5 Hz, 2H), 3.06 ppm (s, 3H).

Acknowledgements

[1] a) *Polymers for Second-Order Nonlinear Optics* (Eds.: G. A. Lindsay, K. D. Singer), ACS Symposium Series 601, American Chemical Society, Washington, DC, **1995**; b) *Molecular Nonlinear Optics* (Ed.: J. Zyss), Academic Press, New York, **1994**; c) *Optical Nonlinearities in Chemistry*, (Ed.: D. M. Burland), *Chem. Rev.* **1994**, *94*, 1–278; d) P. N. Prasad, D. J. Williams, *Introduction to Nonlinear Optical Effects in Molecules and Polymers*, Wiley, New York, **1991**.

[2] S. R. Marder, J. W. Perry, G. Bourhill, C. B. Gorman, B. G. Tiemann, K. Mansour, *Science* **1993**, *261*, 186–189.

[3] a) R. Wortmann, C. Poga, R. J. Twieg, C. Geletneky, *J. Chem. Phys.* **1996**, *105*, 10637–10647; b) R. Wortmann, C. Glania, P. Kramer, K. Lukaszuk, R. Matschiner, R. J. Twieg, F. You, *Chem. Phys.* **1999**, *245*, 107–120.

[4] a) M. Barzoukas, C. Runser, A. Fort, M. Blanchard-Desce, *Chem. Phys. Lett.* **1996**, *257*, 531–537; b) W. H. Thompson, M. Blanchard-Desce, V. Alain, J. Muller, A. Fort, M. Barzoukas, J. T. Hynes, *J. Phys. Chem.* **1999**, *103*, 3766–3771; c) G. Bourhill, J. L. Bredas, L. T. Cheng, S. R. Marder, F. Meyers, J. W. Perry, B. G. Tiemann, *J. Am. Chem. Soc.* **1994**, *116*, 2619–2620; d) C. Maertens, C. Detrembleur, P. Dubois, R. Jerome, C. Boutton, A. Persoons, T. Kogej, J. L. Bredas, *Chem. Eur. J.* **1999**, *5*, 369–380.

[5] a) S. R. Marder, C. B. Gorman, B. G. Tiemann, L. T. Cheng, *J. Am. Chem. Soc.* **1993**, *115*, 3006–3007; b) G. U. Bublitz, R. Ortiz, C. Runser, A. Fort, M. Barzoukas, S. R. Marder, S. G. Boxer, *J. Am. Chem. Soc.* **1997**, *119*, 2311–2312.

[6] A. Abbotto, S. Bradamante, A. Facchetti, G. A. Pagani, *J. Org. Chem.* **1997**, *62*, 5755–5765.

[7] a) A. Abbotto, S. Bradamante, A. Facchetti, G. A. Pagani, I. Ledoux, J. Zyss, *Mater. Res. Soc. Symp. Proc.* **1998**, *488*, 819–822; b) A. Abbotto, S. Bradamante, A. Facchetti, G. A. Pagani, L. Yuan, P. N. Prasad, *Gazz. Chim. Ital.* **1997**, *127*, 165–166.

[8] a) A. Painelli, *Chem. Phys.* **1999**, *245*, 185–197; b) R. Cammi, B. Mennucci, J. Tomasi, *J. Am. Chem. Soc.* **1998**, *120*, 8834–8847; c) I. D. L. Albert, T. J. Marks, M. A. Ratner, *J. Phys. Chem.* **1996**, *100*, 9714–9725; d) R. Wortmann, D. Bishop, *J. Chem. Phys.* **1998**, *108*, 1001–1007.

[9] a) C. Dehu, F. Meyers, E. Hendrickx, K. Clays, A. Persoons, S. R. Marder, J. L. Bredas, *J. Am. Chem. Soc.* **1995**, *117*, 10127–10128; b) C. Runser, A. Fort, M. Barzoukas, C. Combellas, C. Suba, A. Thiebault, R. Graff, J. P. Kintzinger, *Chem. Phys.* **1995**, *193*, 309–319.

[10] A. R. Katritzky in *Handbook of Heterocyclic Chemistry*, Pergamon Press, Oxford, **1983**.

[11] S. Bradamante, A. Facchetti, G. A. Pagani, *J. Phys. Org. Chem.* **1997**, *10*, 514–524.

[12] I. D. L. Albert, T. J. Marks, M. A. Ratner, *J. Am. Chem. Soc.* **1997**, *119*, 6575–6582.

[13] a) C. W. Dirk, H. E. Katz, M. L. Schilling, L. A. King, *Chem. Mater.* **1990**, *2*, 700–705; b) K. Y. Wong, A. K.-Y. Jen, V. P. Rao, *Phys. Rev. A* **1994**, *49*, 3077–3080.

[14] a) J. O. Morley, R. M. Morley, R. Docherty, M. H. Charlton, *J. Am. Chem. Soc.* **1997**, *119*, 10192–10202; b) J. Abe, Y. Shirai, N. Nemoto, F. Miyata, Y. Nagase, *J. Phys. Chem. B* **1997**, *101*, 576–582; c) M. Szablewski, P. R. Thomas, A. Thornton, D. Bloor, G. H. Cross, J. M. Cole, J. A. K. Howard, M. Malagoli, F. Meyers, J. L. Bredas, W. Wenseleers, E. Goovaerts, *J. Am. Chem. Soc.* **1997**, *119*, 3144–3154; d) G. J. Ashwell, R. C. Hargreaves, C. E. Baldwin, G. S. Bahra, C. R. Brown, *Nature* **1992**, *357*, 393–395; e) A. Fort, C. Runser, M. Barzoukas, C. Combellas, C. Suba, A. Thiebault, *SPIE Proceed.* **1994**, *2285*, 2–10.

[15] A. Abbotto, S. Bradamante, G. A. Pagani, *J. Org. Chem.* **2001**, *66*, 8883–8892.

[16] J. J. Wolff, R. Wortmann, *Adv. Phys. Org. Chem.* **1999**, *32*, 121–217.

[17] a) W. Liptay in *Excited States, Vol. 1. Dipole Moments and Polarizabilities of Molecules in Excited Electronic States* (Ed.: E. C. Lim), Academic Press, New York, **1974**, pp. 129–229; b) R. Wortmann, K. Elich, S. Lebus, W. Liptay, P. Borowicz, A. Grabowska, *J. Phys. Chem.* **1992**, *96*, 9724–9730.

[18] J. March, *Advanced Organic Chemistry*, Wiley, New York, **1985**, p. 41.

[19] a) V. Alain, M. Blanchard-Desce, I. Ledoux-Rak, J. Zyss, *Chem. Commun.* **2000**, *5*, 353–354; b) F. Würthner, S. Yao, R. Wortmann, *Polym. Mater. Sci. Eng.* **2000**, *83*, 186–187; c) V. Alain, A. Fort, M. Barzoukas, C.-T. Chen, M. Blanchard-Desce, S. R. Marder, J. W. Perry, *Inorg. Chim. Acta* **1996**, *242*, 43–49.

[20] C. Reichardt, *Solvent Effects in Organic Chemistry*, Verlag Chemie, New York, **1979**, Chapter 6.

[21] A preliminary investigation into the concentration-dependent UV/Vis absorption of **1b** and **2b** in dioxane has shown that the normalized absorption of the lowest energy band increases with decreasing concentration, while that of the highest energy band decreases correspondingly, supporting the hypothesis that the former band could be attributable to the monomeric species. A vibronic structure of the spectra at higher dilution was also observed. A detailed UV/Vis, NMR and computational investigation into aggregates is under way and will be reported in due course.

[22] F. Würthner, S. Yao, T. Debaerdemaeker, R. Wortmann, *J. Am. Chem. Soc.* **2002**, *124*, 9431–9447.

[23] a) S. Di Bella, G. Lanza, I. Fragalà, S. Yitzchaik, M. A. Ratner, T. J. Marks, *J. Am. Chem. Soc.* **1997**, *119*, 3003–3006; b) J. Zheng, C. H. Huang, Y. Y. Huang, D. G. Wu, T. X. Wei, A. C. Yu, X. S. Zhao, *New J. Chem.* **2000**, *24*, 317–321; c) J. L. Bredas, F. Meyers, *Nonlinear Opt.* **1991**, *1*, 119–123.

[24] We have previously defined the charge demand c_X of a substituent group X as the fraction of π-charge withdrawn from an adjacent charged sp^2-carbon atom, and have subsequently used charge demands as a measure of the capacity of group X to delocalize positive or negative charge:a) S. Bradamante, G. A. Pagani, *J. Chem. Soc. Perkin Trans. 2* **1986**, 1035–1045; b) S. Bradamante, G. A. Pagani, *Pure Appl. Chem.* **1989**, *61*, 709–716; c) E. Barchiesi, S. Bradamante, R. Ferraccioli, G. A. Pagani, *J. Chem. Soc. Perkin Trans. 2* **1990**, 375–383.

[25] a) A. Abbotto, S. Bradamante, G. A. Pagani, *J. Org. Chem.* **1993**, *58*, 449–455; b) A. Abbotto, V. Alanzo, S. Bradamante, G. A. Pagani, *J. Chem. Soc. Perkin Trans. 2* **1991**, 481–488; c) A. Abbotto, S. Bradamante, G. A. Pagani, *J. Org. Chem.* **1993**, *58*, 444–448; d) C. Gatti, A. Ponti, A. Gamba, G. A. Pagani, *J. Am. Chem. Soc.* **1992** *114*, 8634–8644.

[26] G. Scheibe, W. Seiffert, G. Hohlneicher, C. Jutz, H. J. Springer, *Tetrahedron Lett.* **1966**, 5053–5059.

[27] R. Radeglia, S. Dähne, *J. Mol. Struct.* **1970**, *5*, 399–411.

[28] M. Blanchard-Desce, V. Alain, P. V. Bedworth, S. R. Marder, A. Fort, C. Runser, M. Barzoukas, S. Lebus, R. Wortmann, *Chem. Eur. J.* **1997**, *3*, 1091–1104.

[29] A. Mishra, R. K. Behera, P. K. Behera, B. K. Mishra, G. B. Behera, *Chem. Rev.* **2000**, *100*, 1973–2011.

[30] F. Steybe, F. Effenberger, P. Krämer, C. Glania, R. Wortmann, *Chem. Phys.* **1997**, *219*, 317–331.

[31] a) S. Beckmann, K.-H. Etzbach, P. Kramer, K. Lucaszuk, A. Matschiner, A. J. Schmidt, P. Schumacher, R. Sens, G. Seibold, R. Wortmann, F. Würthner, *Adv. Mater.* **1999**, *11*, 536–541; b) F. Würthner, C. Thalacker, R. Matschiner, K. Lukaszuk, R. Wortmann, *Chem. Commun.* **1998**, 1739–1740.

[32] a) F. Würthner, R. Wortmann, R. Matschiner, K. Lukaszuk, K. Meerholz, Y. DeNardin, R. Bittner, C. Bräuchle, R. Sens, *Angew. Chem.* **1997**, *109*, 2933–2936; *Angew. Chem. Int. Ed. Engl.* **1997**, *36*, 2765–2768; b) K. Meerholz, Y. DeNardin, R. Bittner, R. Wortmann, F. Würthner, *Appl. Phys. Lett.* **1998**, *73*, 4–6; c) F. Würthner, C. Legrand, E. Mecher, K. Meerholz, R. Wortmann, *Polym. Mat. Sci. Eng.* **1999**, *80*, 252–254; d) R. Wortmann, F. Würthner, A. Sautter, K. Lukaszuk, R. Matschiner, K. Meerholz, *SPIE Proceed.* **1998**, *3471*, 41–49.

[33] GAUSSIAN 98, Revision A.9, M. J. Frisch, G. W. Trucks, H. B. Schlegel, G. E. Scuseria, M. A. Robb, J. R. Cheeseman, V. G. Zakrzewski, J. A. Montgomery Jr., R. E. Stratmann, J. C. Burant, S. Dapprich, J. M. Millam, A. D. Daniels, K. N. Kudin, M. C. Strain, O. Farkas, J. Tomasi, V. Barone, M. Cossi, R. Cammi, B. Mennucci, C. Pomelli, C. Adamo, S. Clifford, J. Ochterski, G. A. Petersson, P. Y. Ayala, Q. Cui, K. Morokuma, D. K. Malick, A. D. Rabuck, K. Raghavachari, J. B. Foresman, J. Cioslowski, J. V. Ortiz, A. G. Baboul, B. B. Stefanov, G. Liu, A. Liashenko, P. Piskorz, I. Komaromi, R. Gomperts, R. L. Martin, D. J. Fox, T. Keith, M. A. Al-Laham, C. Y. Peng, A. Nanayakkara, M. Challacombe, P. M. W. Gill, B. Johnson, W. Chen, M. W. Wong, J. L. Andres, C. Gonzalez, M. Head-Gordon, E. S. Replogle, J. A. Pople, Gaussian, Inc., Pittsburgh PA, 1998.

[34] Computations were partially carried out at the Cineca Supercomputer Center in Bologna (Italy) on SGI Origin 3800 and IBM SP RS/6000 Power3 machines.

[35] Full-geometry optimizations and energy calculations at the B3LYP/6–31G*//B3LYP/6–31G* level of theory were carried out for compound **1c** (C_s symmetry) in the gas phase and in dioxane, CHCl$_3$ and DMF. DFT-computed dipole moment values are included in Table 4.

[36] a) L. Onsager, *J. Am. Chem. Soc.* **1936**, *58*, 1486–1493; b) M. W. Wong, M. J. Frisch, K. B. Wiberg, *J. Am. Chem. Soc.* **1991**, *113*, 4776–4782.

[37] We are aware that the Onsager reaction field model should be used only under the strict assumption that all chromophores are spherical in shape, a case clearly not applicable here. Recent work by Dalton and Robinson on a Monte Carlo treatment of the electrooptic activity of dipolar chromophores has indeed pointed out the effect of spherical versus ellipsoidal shapes, the latter fitting experimental data more closely (B. H. Robinson, L. R. Dalton, *J. Phys. Chem.* **2000**, *104*, 4785–4795). Unfortunately, other theoretical models available in the Gaussian package, such as the polarized continuum model (PCM), in which the cavity is defined as the sum of a series of interlocking spheres, or the alternative self-consistent isodensity polarized continuum model (SCI-PCM), did not satisfy convergence criteria during geometry optimizations even of the smallest system **1c**. It became evident that the Onsager model was the only method able to satisfy convergence criteria completely for the full set of compounds and solvents to be considered in this study. Such a simplification could be responsible for a certain degree of deviation from experimental data. However, we believe that the overall good, and sometimes very good, agreement with different experimental data do validate this computational approach.

[38] Such a decision was based on semiempirical (PM3) computations showing that the C_1 and C_s geometries have very similar energies (difference is below 1 kcal mol^{-1}) and that deviation from planarity in the more stable C_1 structure is not significant.

[39] A. E. Reed, R. B. Weinstock, F. Weinhold, *J. Chem. Phys.* **1985**, *83*, 735–746.

[40] Gaussian NBO. Version 3.1 (as incorporated in the GAUSSIAN 98 package).

[41] a) J. Gerratt, I. M. Mills, *J. Chem. Phys.* **1968**, *49*, 1730–1739; b) G. J. B. Hurst, M. Dupuis, E. Clementi, *J. Chem. Phys.* **1988**, *89*, 385–395; c) H. Sekino, R. J. Bartlett, *J. Chem. Phys.* **1991**, *94*, 3665–3669; d) S. P. Karna, M. Dupuis, *J. Comput. Chem.* **1991**, *12*, 487–504.

[42] D. R. Kanis, M. A. Ratner, T. J. Marks, *Chem. Rev.* **1994**, *94*, 195–242.

[43] a) D. A. Kleinman, *Phys. Rev.* **1962**, *126*, 1977–1979; b) C. Bosshard, K. Sutter, P. Prêtre, J. Hulliger, M. Flörsheimer, P. Kaatz, P. Günter, *Organic Nonlinear Optical Materials - Advances in Nonlinear Optics*, Vol. 1 (Eds.: A. F. Garito, F. Kajzar), Gordon and Breach, Basel, **1995**.

[44] A. Willets, J. E. Rice, D. M. Burland, D. P. Shelton, *J. Chem. Phys.* **1992**, *97*, 7590–7599.

[45] a) *Photonic Polymer Systems* (Eds.: D. L. Wise, G. E. Wnek, D. J. Trantolo, T. M. Cooper, J. D. Gresser), Marcel Dekker, New York, **1998**; b) L. R. Dalton, A. W. Harper, R. Ghosn, W. H. Steir, M. Ziari, H. Fetterman, Y. Shi, R. V. Mustacich, A. K.-Y. Jen, K. J. Shea, *Chem. Mater.* **1995**, *7*, 1060–1081.

[46] P. Innocenzi, E. Miorin, G. Brusatin, A. Abbotto, L. Beverina, G. A. Pagani, M. Casalboni, F. Sarcinelli, R. Pizzoferrato, *Chem. Mater.* **2002**, *14*, 3758–3766.

[47] S. Gronowitz, S. Liljefors, *Chem. Scr.* **1979**, *13*, 39–45.

[48] U. Möller, D. Cech, F. Schubert, *Liebigs Ann. Chem.* **1990**, 1221–1225.